The International Pulsar Timing Array: First data release

J. P. W. Verbiest,[1,2]★ L. Lentati,[3] G. Hobbs,[4] R. van Haasteren,[5] P. B. Demorest,[6]
G. H. Janssen,[7] J.-B. Wang,[8] G. Desvignes,[2] R. N. Caballero,[2] M. J. Keith,[9]
D. J. Champion,[2] Z. Arzoumanian,[10] S. Babak,[11] C. G. Bassa,[7] N. D. R. Bhat,[12]
A. Brazier,[13,14] P. Brem,[11] M. Burgay,[15] S. Burke-Spolaor,[6] S. J. Chamberlin,[16]
S. Chatterjee,[14,17] B. Christy,[18] I. Cognard,[19,20] J. M. Cordes,[17] S. Dai,[4,21]
T. Dolch,[22,14,17] J. A. Ellis,[5] R. D. Ferdman,[23] E. Fonseca,[24] J. R. Gair,[25]
N. E. Garver-Daniels,[26] P. Gentile,[26] M. E. Gonzalez,[27] E. Graikou,[2] L. Guillemot,[19,20]
J. W. T. Hessels,[7,28] G. Jones,[29] R. Karuppusamy,[2] M. Kerr,[4] M. Kramer,[2,9] M.
T. Lam,[17] P. D. Lasky,[30] A. Lassus,[2] P. Lazarus,[2] T. J. W. Lazio,[5] K. J. Lee,[31]
L. Levin,[26,9] K. Liu,[2] R. S. Lynch,[32] A. G. Lyne,[9] J. Mckee,[9]
M. A. McLaughlin,[26] S. T. McWilliams,[26] D. R. Madison,[33] R. N. Manchester,[4]
C. M. F. Mingarelli,[34,2] D. J. Nice,[35] S. Osłowski,[1,2] N. T. Palliyaguru,[36]
T. T. Pennucci,[37] B. B. P. Perera,[9] D. Perrodin,[15] A. Possenti,[15] A. Petiteau,[38]
S. M. Ransom,[33] D. Reardon,[30,4] P. A. Rosado,[39] S. A. Sanidas,[28] A. Sesana,[40]
G. Shaifullah,[2,1] R. M. Shannon,[4,12] X. Siemens,[41] J. Simon,[41] R. Smits,[7] R. Spiewak,[41]
I. H. Stairs,[24] B. W. Stappers,[9] D. R. Stinebring,[42] K. Stovall,[43]
J. K. Swiggum,[26] S. R. Taylor,[5] G. Theureau,[19,20,44] C. Tiburzi,[2,1] L. Toomey,[4]
M. Vallisneri,[5] W. van Straten,[39] A. Vecchio,[40] Y. Wang,[45] L. Wen,[46] X. P. You,[47]
W. W. Zhu[2] and X.-J. Zhu[46]

Affiliations are listed at the end of the paper

ABSTRACT

The highly stable spin of neutron stars can be exploited for a variety of (astro)physical investigations. In particular, arrays of pulsars with rotational periods of the order of milliseconds can be used to detect correlated signals such as those caused by gravitational waves. Three such 'pulsar timing arrays' (PTAs) have been set up around the world over the past decades and collectively form the 'International' PTA (IPTA). In this paper, we describe the first joint analysis of the data from the three regional PTAs, i.e. of the first IPTA data set. We describe the available PTA data, the approach presently followed for its combination and suggest improvements for future PTA research. Particular attention is paid to subtle details (such as underestimation of measurement uncertainty and long-period noise) that have often been ignored but which become important in this unprecedentedly large and inhomogeneous data set. We identify and describe in detail several factors that complicate IPTA research and provide recommendations for future pulsar timing efforts. The first IPTA data release presented here (and available online) is used to demonstrate the IPTA's potential of improving upon gravitational-wave limits

★ E-mail: verbiest@physik.uni-bielefeld.de

placed by individual PTAs by a factor of ∼2 and provides a 2σ limit on the dimensionless amplitude of a stochastic gravitational-wave background of 1.7×10^{-15} at a frequency of $1\,\mathrm{yr}^{-1}$. This is 1.7 times less constraining than the limit placed by Shannon et al., due mostly to the more recent, high-quality data they used.

Key words: methods: data analysis – pulsars: general.

1 INTRODUCTION

The stable and regular rotation of pulsars, combined with their lighthouse-like radiation beams enable a wide variety of pulsar timing experiments of (astro)physical interest (see Lorimer & Kramer 2005, for an overview). Of particular interest is the use of pulsar timing arrays (PTAs) to detect correlated signals, such as those caused by gravitational waves (GWs). In the following, the technique of pulsar timing is explained in some detail (Section 1.1), followed by the potential sources of GWs that our experiment might be expected to be sensitive to (Section 1.2). The sensitivity scaling laws for such GW-detection efforts are described in Section 1.3 and this provides a clear case for combining data from as many telescopes as possible, which is the subject of this paper, introduced in Section 1.4.

1.1 Pulsar timing

The process of pulsar timing is fundamentally dependent on an accurate description of everything that affects the times of arrival (ToAs) of the pulsed radiation at the telescope. In addition to a time standard and the Solar-system ephemerides (which predict the positions and masses of the Solar-system bodies at any given point in time, to the degree this information is available), pulsar timing requires knowledge of the pulsar's spin and spin-down, its position and proper motion, its distance, the number of dispersing electrons in the interstellar medium along the propagation path of the radio waves and (unless the pulsar is solitary) multiple orbital parameters. All of these parameters are included in a so-called 'timing model', which can be used to predict the phase of the pulsar's periodic signal at any point in time. For a full description of the technique of pulsar timing, we refer the interested reader to Lorimer & Kramer (2005) and for a complete derivation of the formulae included in pulsar timing models, Edwards, Hobbs & Manchester (2006) is recommended. In the following, we will merely highlight the aspects that are directly relevant to the further analysis presented in this paper.

To determine the arrival times from the observations, a high signal-to-noise ratio (S/N) 'template' profile (i.e. phase-resolved pulse shape) is constructed through coherent addition of the highest quality data. This template (or an analytic version derived from it) is then used as a phase reference against which all other observations are timed through cross-correlation (Taylor 1992). The differences between the measured ToAs and those predicted by the timing model are the 'timing residuals', which are the unmodelled difference between the observations and the theory. It is the investigation of these timing residuals that allows additional science (i.e. all the science that is not yet included in the timing model) to be derived.

The amount of information that can be derived from the timing residuals of any given pulsar varies strongly. In particular, some binary pulsars are more interesting as they may yield information on the binary system, such as the pulsar and companion masses, whereas solitary pulsars can typically at best provide their spin period, spin-down, parallax and proper motion. Non-pulsar-specific correlated signals, however, should be encoded in the timing residuals of all pulsars. Three such signals are of particular interest to PTA experiments (Foster & Backer 1990; Tiburzi et al. 2016).

(i) A monopolar signal, which affects all pulsars equally, would be caused by an error in the Earth-based time standards.[1] Recently, Hobbs et al. (2012) used PTA data to constrain this signal.

(ii) A dipolar signal, which would be caused by an imperfection in our models of the Solar system. Since the ToAs are necessarily corrected for the Earth's motion around the Solar-system barycentre, incomplete information on the masses and positions of Solar-system bodies would cause errors in the timing residuals. Champion et al. (2010) made a first attempt at measuring such a signal in PTA data.

(iii) A quadrupolar signal, as would be caused by GWs, which distort space–time in a quadrupolar fashion and therefore affect the ToAs of pulsar signals in a quadrupolar way (Hellings & Downs 1983).[2] An overview of recent analyses on such signals is given in Section 1.2.

In order to detect the extremely weak effects listed above in the timing residuals, it is important to have very high precision and accuracy in the measured ToAs. Two sources of white noise in the pulse observations determine this precision and accuracy. The first of these is radiometer noise, which affects ToA precision and can be quantified (in the case of a simple Gaussian or rectangular pulse shape) with the radiometer equation for pulsar timing (after Lorimer & Kramer 2005):

$$\sigma_{\mathrm{Radiom}} = k \frac{S_{\mathrm{sys}} P \delta^{3/2}}{S_{\mathrm{mean}} \sqrt{t_{\mathrm{int}} n_{\mathrm{pol}} \Delta f}}, \tag{1}$$

with k a correction factor accounting for digitization losses ($k \approx 1$ for modern systems, but for some of the older, one- or two-bit systems $k \approx 1.2$); $S_{\mathrm{sys}} = T_{\mathrm{sys}}/G = 2k_{\mathrm{B}}T_{\mathrm{sys}}/A_{\mathrm{eff}}$ the system equivalent flux density which depends on the system temperature T_{sys}, the telescope's effective collecting area A_{eff} and Boltzmann's constant, k_{B}. P is the pulse period of the pulsar, $\delta = W/P$ is the pulsar's duty cycle (pulse width W divided by pulse period), S_{mean} is the flux density of the pulsar averaged over its pulse period, n_{pol} is the number of polarizations observed and t_{int} and Δf are, respectively, the duration and bandwidth of the observation. The second white-noise contribution is pulse-phase jitter, also known as SWIMS (Osłowski et al. 2011, 2013) and affecting both the ToA accuracy and precision. SWIMS are relevant in any system that has sufficient sensitivity to detect individual pulses from pulsars, as it quantifies the stability of pulsar pulse shapes on short time-scales, given by

$$\sigma_{\mathrm{Jitter}} \propto \frac{f_{\mathrm{J}} W_{\mathrm{eff}} \left(1 + m_{\mathrm{I}}^2\right)}{\sqrt{N_{\mathrm{p}}}}, \tag{2}$$

---

[1] See Khmelnitsky & Rubakov (2014) and Porayko & Postnov (2014) however for a potentially different origin.

[2] Hellings & Downs (1983) also showed that the effect of the GWs on the timing is fully characterized by their effect at the time the pulsar signal is emitted (the so-called 'pulsar term') and at the time the signal is received (the so-called 'Earth term'). In the absence of highly precise information on the distances of the pulsars in the array, only the Earth term is correlated, in which case the GW effect is not a purely quadrupolar signal, but a quadrupolar signal with an equally strong white-noise component.

Table 1. Sources of IPTA data. For each regional PTA the telescopes used in the current data set are listed, along with the typical time between observations, the number of pulsars observed at each telescope and the observing frequencies used (rounded to the nearest 100 MHz and limited to a single band per GHz interval). The final two columns give the MJD range over which observations are included in the current combination. The Kaspi, Taylor & Ryba (1994) data set is not part of a PTA as such, but refers to the publicly available data sets on PSRs J1857+0943 and J1939+2134, which have also been included in the combined IPTA data. Note that all three PTAs are ongoing efforts that continue to extend their data sets. Because the present IPTA combination did not run in parallel to these individual efforts and took significantly more time than a data combination at the level of an individual PTA, these constituent data sets are often significantly outdated. A follow-up effort to create a second IPTA data combination containing all the most recent data available to the three individual PTAs is ongoing.

PTA	Telescope (code)	Typical cadence (weeks)	Number of pulsars	Observing frequencies (GHz)	Earliest date (MJD, Gregorian)	Latest date (MJD, Gregorian)
EPTA	Effelsberg (EFF)	4	18	1.4, 2.6	50360 (1996 Oct 04)	55908 (2011 Dec 13)
	Lovell (JBO)	3	35	1.4	54844 (2009 Jan 13)	56331 (2013 Feb 08)
	Nançay Radio Telescope (NRT)	2	42	1.4, 2.1	47958 (1990 Mar 08)	55948 (2012 Jan 22)
	Westerbork (WSRT)	4	19	0.3, 1.4, 2.2	51386 (1999 Jul 27)	55375 (2010 Jun 28)
NANOGrav	Green Bank Telescope (GBT)	4	10	0.8, 1.4	53216 (2004 Jul 30)	55122 (2009 Oct 18)
	Arecibo (AO)	4	8	0.3, 0.4, 1.4, 2.3	53343 (2004 Dec 04)	55108 (2009 Oct 04)
Zhu et al. (2015)	GBT & AO	2	1	0.8, 1.4, 2.3	48850 (1992 Aug 16)	56598 (2013 Nov 02)
PPTA	Parkes (PKS)	2	20	0.6, 1.4, 3.1	49373 (1994 Jan 21)	56592 (2013 Oct 27)
Kaspi et al. (1994)	Arecibo (AO)	2	2	1.4, 2.3	46436 (1986 Jan 06)	48973 (1992 Dec 17)

with f_J the jitter parameter, which needs to be determined experimentally (Liu et al. 2012; Shannon et al. 2014); W_{eff} the pulse width; $m_I = \sigma_E/\mu_E$ the modulation index, defined by the mean (μ_E) and standard deviation (σ_E) of the pulse-energy distribution; and $N_p = t_{int}/P$ the number of pulses in the observation, which equals the total observing time divided by the pulse period.

Consequently, the highest precision timing efforts ideally require rapidly rotating pulsars ($P \lesssim 0.03$ s) with high relatively flux densities ($S_{1.4\,GHz} \gtrsim 0.5$ mJy) and narrow pulses ($\delta \lesssim 20$ per cent) are observed at sensitive (A_{eff}/T_{sys}) telescopes with wide-bandwidth receivers (Δf) and for long integration times ($t_{int} \gtrsim 30$ min).

1.2 GW detection with pulsar timing

In order to detect the correlated signals in pulsar timing data, an array of millisecond pulsars (MSPs) must be observed with large, sensitive telescopes. Such a 'PTA'[3] (Romani 1989; Foster & Backer 1990) has currently been set up in three different places. Specifically, the Australian Parkes PTA (PPTA; Manchester et al. 2013) is centred on the Parkes radio telescope (PKS); the European PTA (EPTA; Desvignes et al. 2016) uses the five[4] major European centimetre-wavelength telescopes (see Table 1 for details); and the North-American Nanohertz Observatory for GWs (NANOGrav; Arzoumanian et al. 2015) uses the Robert C. Byrd Green Bank Telescope (GBT) and the 305-m William E. Gordon Telescope of the Arecibo Observatory (AO). Combined, these three PTAs form the International PTA (or IPTA, as previously described by Hobbs et al. 2010a; Manchester & IPTA 2013) and presently observe 49 pulsars (see Table 2 for details) in the quest for the aforementioned correlated signals and for GWs in particular.

The search for GW signals in pulsar timing data is pursued along several lines, according to the types of predicted GW sources. In

the past (see e.g. Hellings & Downs 1983; Foster & Backer 1990; Kaspi et al. 1994; Jenet et al. 2005), isotropic and incoherent GW backgrounds (GWB) were considered in a pulsar timing context. Such a GWB could arise in three different ways. First, it could be the gravitational equivalent to the cosmic microwave background: a GWB arising from the era of graviton decoupling in the early Universe [Grishchuk 2005; Boyle & Buonanno 2008 or from phase transitions in the early Universe (Schwaller 2015)]. Secondly, various processes involving cosmic strings could cause a GWB at frequencies detectable by PTAs (Sanidas, Battye & Stappers 2012, and reference therein). Finally, hierarchical galaxy-formation models predict a large number of supermassive black hole (SMBH) binaries in the Universe's history. This population would produce a GWB of particular astrophysical interest and its predicted amplitude and frequency range may well lie within reach of current PTA sensitivity (Rajagopal & Romani 1995; Sesana 2013).

In addition to stochastic sources of GWs, several types of single sources could be detectable by PTA efforts as well. Clearly nearby SMBH binaries would be detectable if they stand out above the aforementioned background (Sesana, Vecchio & Volonteri 2009), but in addition to those, bursts of GWs might be detected as well, arising from a periastron passage in a highly eccentric SMBH binary (Finn & Lommen 2010), cusps in cosmic strings (Damour & Vilenkin 2000) or single SMBH merger events (Seto 2009; Pshirkov, Baskaran & Postnov 2010; van Haasteren & Levin 2010). Interestingly, in the case of a single SMBH merger, the merger event itself is likely undetectable to PTAs, but its gravitational memory effect (Favata 2009) might be detectable.

At present, the most constraining limit from pulsar timing on the stochastic GWB, is a 95 per cent-confidence upper limit of 1.0×10^{-15} on the dimensionless strain amplitude,[5] that was obtained by Shannon et al. (2015) and based on data from the PPTA. Competitive limits of 1.5×10^{-15} and 3×10^{-15} have been placed by Arzoumanian et al. (2016) and Lentati et al. (2015), respectively,

---

[3] Where originally the acronym 'PTA' was purely defined as the set of pulsars that comprise the experiment, more recently the same acronym has been used to refer to the collaborations that carry out these experiments. We continue this convention of having one acronym to refer to both the set of pulsars and the scientific collaboration.
[4] The Sardinia Radio Telescope in Italy is also part of the EPTA collaboration, but had not yet commenced routine scientific observations during the timespan covered by the data presented in this work.

[5] Note that all limits quoted here are at a reference frequency of $1\,yr^{-1}$ or 32 nHz and where needed assume a spectral index for the characteristic strain spectrum of $-2/3$, as expected from an incoherent superposition of SMBH binary signals.

Table 2. The pulsars in the first IPTA data release with their basic properties. Given are the name in the J2000 system (note the following pulsars also have B1950 names: PSRs J1824−2452A, J1857+0943, J1939+2134 and J1955+2908 are, respectively, known as PSRs B1821−24A, B1855+09, B1937+21 and B1953+29), the pulse period in milliseconds, the orbital period in days, the dispersion measure in cm^{-3} pc, the flux at 1.4 GHz in mJy (if available) and the most likely distance in kpc, either from distance measurements compiled by Verbiest et al. (2012) or (indicated by †) from the Galactic electron density model of Cordes & Lazio (2002), assuming a 20 per cent uncertainty. The next three columns indicate by 'X' the PTAs in which the pulsar is observed and the final column gives the relevant references for the given data, typically including the discovery paper, the most recent timing analysis and where relevant a paper with the very long baseline interferometry astrometry or flux density measurement. The references are as follows: (1) Lommen et al. (2000), (2) Abdo et al. (2009), (3) Lommen et al. (2006), (4) Bailes et al. (1994), (5) Abdo et al. (2010), (6) Hobbs et al. (2004b), (7) Toscano et al. (1998), (8) Navarro et al. (1995), (9) Kramer et al. (1998), (10) Du et al. (2014), (11) Verbiest & Lorimer (2014), (12) Johnston et al. (1993), (13) Verbiest et al. (2008), (14) Manchester et al. (2013), (15) Deller et al. (2008), (16) Burgay et al. (2006), (17) Lorimer et al. (1995), (18) Verbiest et al. (2009), (19) Camilo et al. (1996b), (20) Splaver et al. (2002), (21) Bailes et al. (1997), (22) Lundgren, Zepka & Cordes (1995), (23) Nice et al. (2005), (24) Nicastro et al. (1995), (25) Lazaridis et al. (2009), (26) Hotan, Bailes & Ord (2006), (27) Jacoby et al. (2007), (28) Lorimer et al. (1996), (29) Löhmer et al. (2005), (30) Foster, Wolszczan & Camilo (1993), (31) Edwards & Bailes (2001), (32) Janssen et al. (2010), (33) Jacoby (2004), (34) Freire et al. (2012), (35) Stairs et al. (2005), (36) Faulkner et al. (2004), (37) Lorimer et al. (2006), (38) Lyne et al. (1987), (39) Hobbs et al. (2004a), (40) Ferdman et al. (2010), (41) Gonzalez et al. (2011), (42) Segelstein et al. (1986), (43) Frail & Weisberg (1990), (44) Jacoby et al. (2003), (45) Toscano et al. (1999), (46) Backer et al. (1982), (47) Boriakoff, Buccheri & Fauci (1983), (48) Nice, Taylor & Fruchter (1993), (49) Nice, Splaver & Stairs (2001), (50) Ray et al. (1996), (51) Splaver (2004), (52) Camilo (1995), (53) Wolszczan et al. (2000), (54) Camilo, Nice & Taylor (1993), (55) Camilo, Nice & Taylor (1996a), (56) Nice & Taylor (1995), (57) van Straten (2013).

J2000 name	Pulse period (ms)	Orbital period (d)	Dispersion measure (cm^{-3} pc)	Flux density at 1.4 GHz (mJy)	Distance (kpc)	EPTA	NANOGrav	PPTA	Reference(s)
J0030+0451	4.865	–	4.33	0.6	$0.28^{+0.10}_{-0.06}$	X	X		(1, 2, 3)
J0034−0534	1.877	1.6	13.77	0.6	0.5 ± 0.1†	X			(4, 5, 6, 7)
J0218+4232	2.323	2.0	61.25	0.9	$3.2^{+0.9}_{-0.6}$	X			(8, 6, 9, 10, 11)
J0437−4715	5.757	5.7	2.64	149.0	0.156 ± 0.001			X	(12, 13, 14, 15)
J0610−2100	3.861	0.3	60.67	0.4	3.5 ± 0.7†	X			(16)
J0613−0200	3.062	1.2	38.78	2.3	$0.9^{+0.4}_{-0.2}$	X	X	X	(17, 18, 14)
J0621+1002	28.854	8.3	36.60	1.9	1.4 ± 0.3†	X			(19, 20)
J0711−6830	5.491	–	18.41	1.4	0.9 ± 0.2†			X	(21, 18, 14)
J0751+1807	3.479	0.3	30.25	3.2	$0.4^{+0.2}_{-0.1}$	X			(22, 23, 9)
J0900−3144	11.110	18.7	75.70	3.8	0.5 ± 0.1†	X			(16)
J1012+5307	5.256	0.6	9.02	3.0	$0.7^{+0.2}_{-0.1}$	X	X		(24, 25, 9)
J1022+1001	16.453	7.8	10.25	1.5	$0.52^{+0.09}_{-0.07}$	X		X	(19, 18, 57)
J1024−0719	5.162	–	6.49	1.5	$0.49^{+0.12}_{-0.08}$	X		X	(21, 18, 14, 26)
J1045−4509	7.474	4.1	58.17	2.2	$0.23^{+0.17}_{-0.07}$			X	(4, 18, 14)
J1455−3330	7.987	76.2	13.57	1.2	0.5 ± 0.1†	X	X		(17, 6, 7)
J1600−3053	3.598	14.3	52.33	2.4	$2.4^{+0.9}_{-0.6}$	X	X	X	(27, 18, 14)
J1603−7202	14.842	6.3	38.05	4.2	1.2 ± 0.2†			X	(28, 18, 14)
J1640+2224	3.163	175.5	18.43	2.0	1.2 ± 0.2†	X	X		(29, 9)
J1643−1224	4.622	147.0	62.41	5.0	$0.42^{+0.09}_{-0.06}$	X	X	X	(17, 18, 14)
J1713+0747	4.570	67.8	15.99	7.4	$1.05^{+0.06}_{-0.05}$	X	X	X	(30, 18, 14)
J1721−2457	3.497	–	47.76	0.6	1.3 ± 0.3†	X			(31, 32)
J1730−2304	8.123	–	9.62	3.9	0.5 ± 0.1†	X		X	(17, 18, 14)
J1732−5049	5.313	5.3	56.82	1.3	1.4 ± 0.3†			X	(31, 18, 14)
J1738+0333	5.850	0.4	33.77	–	1.5 ± 0.1	X			(33, 34)
J1744−1134	4.075	–	3.14	3.3	0.42 ± 0.02	X	X	X	(21, 18, 14)
J1751−2857	3.915	110.7	42.81	0.1	1.1 ± 0.2†	X			(35)
J1801−1417	3.625	–	57.21	0.2	1.5 ± 0.3†	X			(36, 37)
J1802−2124	12.648	0.7	149.63	0.8	2.9 ± 0.6†	X			(36, 40)
J1804−2717	9.343	11.1	24.67	0.4	0.8 ± 0.2†	X			(28, 6, 9)
J1824−2452A	3.054	–	120.50	1.6	5 ± 1†			X	(38, 18, 14)
J1843−1113	1.846	–	59.96	0.1	1.7 ± 0.3†	X			(39)
J1853+1303	4.092	115.7	30.57	0.4	2.09 ± 0.4†	X	X		(36, 41, 35)
J1857+0943	5.362	12.3	13.30	5.9	0.9 ± 0.2	X	X	X	(42, 18, 14, 43)
J1909−3744	2.947	1.5	10.39	2.6	1.26 ± 0.03	X	X	X	(44, 18, 14)
J1910+1256	4.984	58.5	38.06	0.5	2.3 ± 0.5†	X	X		(36, 41, 35)
J1911+1347	4.626	–	30.99	0.1	1.2 ± 0.2†	X			(28, 45, 9)
J1911−1114	3.626	2.7	30.98	0.5	2.1 ± 0.4†	X			(36, 37)

Table 2 – *continued*

J2000 name	Pulse period (ms)	Orbital period (d)	Dispersion measure ($cm^{-3} pc$)	Flux density at 1.4 GHz (mJy)	Distance (kpc)	EPTA	NANOGrav	PPTA	Reference(s)
J1918−0642	7.646	10.9	26.55	0.6	1.2 ± 0.2†	X	X		(31, 32)
J1939+2134	1.558	–	71.04	13.8	5^{+2}_{-1}	X		X	(46, 18, 14, 43)
J1955+2908	6.133	117.3	104.58	1.1	4.6 ± 0.9†	X	X		(47, 41, 9)
J2010−1323	5.223	–	22.16	1.6	1.0 ± 0.2†	X			(27)
J2019+2425	3.935	76.5	17.20	–	1.5 ± 0.3†	X			(48, 49)
J2033+1734	5.949	56.3	25.08	–	2.0 ± 0.4†	X			(50, 51)
J2124−3358	4.931	–	4.60	2.4	$0.30^{+0.07}_{-0.05}$	X		X	(21, 18, 14)
J2129−5721	3.726	6.6	31.85	1.6	$0.4^{+0.2}_{-0.1}$			X	(28, 18, 14)
J2145−0750	16.052	6.8	9.00	9.3	$0.57^{+0.11}_{-0.08}$	X	X	X	(4, 18, 14)
J2229+2643	2.978	93.0	23.02	0.9	1.5 ± 0.3†	X			(52, 53, 9)
J2317+1439	3.445	2.5	21.91	4.0	0.8 ± 0.2†	X	X		(54, 55, 9)
J2322+2057	4.808	–	13.37	–	0.8 ± 0.2†	X			(48, 56)

based on the NANOGrav and EPTA data. Single-source limits have recently been derived by Babak et al. (2015) from the EPTA data, by Arzoumanian et al. (2014) from the NANOGrav data and by Zhu et al. (2014) from the PPTA data, in all cases showing that all proposed binary SMBH systems are still well below current sensitivity levels. Similar conclusions were reached for GW burst events (Wang et al. 2015). Most recently, Taylor et al. (2015) used the quadrupolar correlation signal to probe the anisotropy and granularity of the background and placed the first constraints on this.

1.3 PTA sensitivity

Because the GWB from SMBH binaries is better-founded and predicted to be stronger than the other backgrounds; and because the burst events are predicted to be extremely rare (Seto 2009; Pshirkov et al. 2010; van Haasteren & Levin 2010), PTA research has so far focused on detecting single SMBH binaries or a stochastic background composed of these. In the low-S/N regime where the GWB contributes less power to the data than the other noise sources outlined in Section 1.1, Siemens et al. (2013) derived that the S/N of a PTA's detection sensitivity scales as

$$S/N \propto NCA^2 T^{13/3}/\sigma^2, \tag{3}$$

where N is the number of pulsars in the array, C the cadence (i.e. the inverse of the typical observing periodicity), A the expected amplitude of the GWB, T the length of the pulsar timing data set and σ the root mean square (rms) of the timing residuals. Clearly the length of the data set is of great importance, as is the timing precision (hence further strengthening the requirement for large, sensitive radio telescopes). In the intermediate regime, where GWs start to stand out beyond the noise, this scaling law changes and the number of pulsars becomes far more relevant:

$$S/N \propto NC^{3/26} A^{3/13} T^{1/2}/\sigma^{3/13}. \tag{4}$$

For single SMBH binary sources, the sensitivity would scale as $A\sqrt{NTC}/\sigma$ (Lee et al. 2011), also strongly dependent on the timing precision. Either single sources or a background of gravitational waves could realistically be expected for the first detection, as demonstrated by Rosado, Sesana & Gair (2015).

The above scaling laws indicate several clear ways of improving the sensitivity of PTAs to GWs in the near future. Specifically, the sensitivity can be improved by adding more pulsars to the array (i.e.

increasing N), as can be achieved particularly through pulsar surveys which discover previously missed MSPs with good potential for high-precision timing (see Fig. 3 and Section 5.2); increasing the observing cadence, C, which can be accomplished through pooling of observing resources, i.e. by combining data from multiple telescopes; increasing the time-span of the observations, T, which can be done through the addition of archival data or continued observing; and improving the timing precision (i.e. lowering σ), which can be done through hardware improvements, increased integration times and bandwidths; and generally by using the most sensitive telescopes available. (More advanced improvements to the analysis method will also strongly impact timing precision. A list of some advances currently under investigation will be presented in Section 5.1.)

A substantial gain in sensitivity could be expected from combining the data sets from the three existing PTAs. This should improve our sensitivity through all factors mentioned above (except the amplitude of the GWs, which is independent of the observing strategy), given existing complementarity between the three PTAs. Such a combination is, however, a technical challenge for a number of reasons that are explained in detail throughout this paper.

1.4 Data combination

In this paper, we provide a detailed analysis of the steps that are involved in an IPTA data-combination project. When combining data from different telescopes and collaborations, in principle the steps should be well defined and straightforward, namely:

(i) concatenate ToAs and merge timing models, or select the best timing model as a starting point;
(ii) insert phase offsets between ToAs of different instruments that have not otherwise been aligned;
(iii) correct ToA uncertainties (which are often underestimated);
(iv) correct time-variable interstellar dispersion;
(v) estimate the covariances between arrival time estimates owing to low-frequency timing noise;
(vi) re-fit the timing model.

However, in practice many of these steps have to be iterated or performed simultaneously, which is often complicated by inconsistencies in the data and lack of (meta)data.
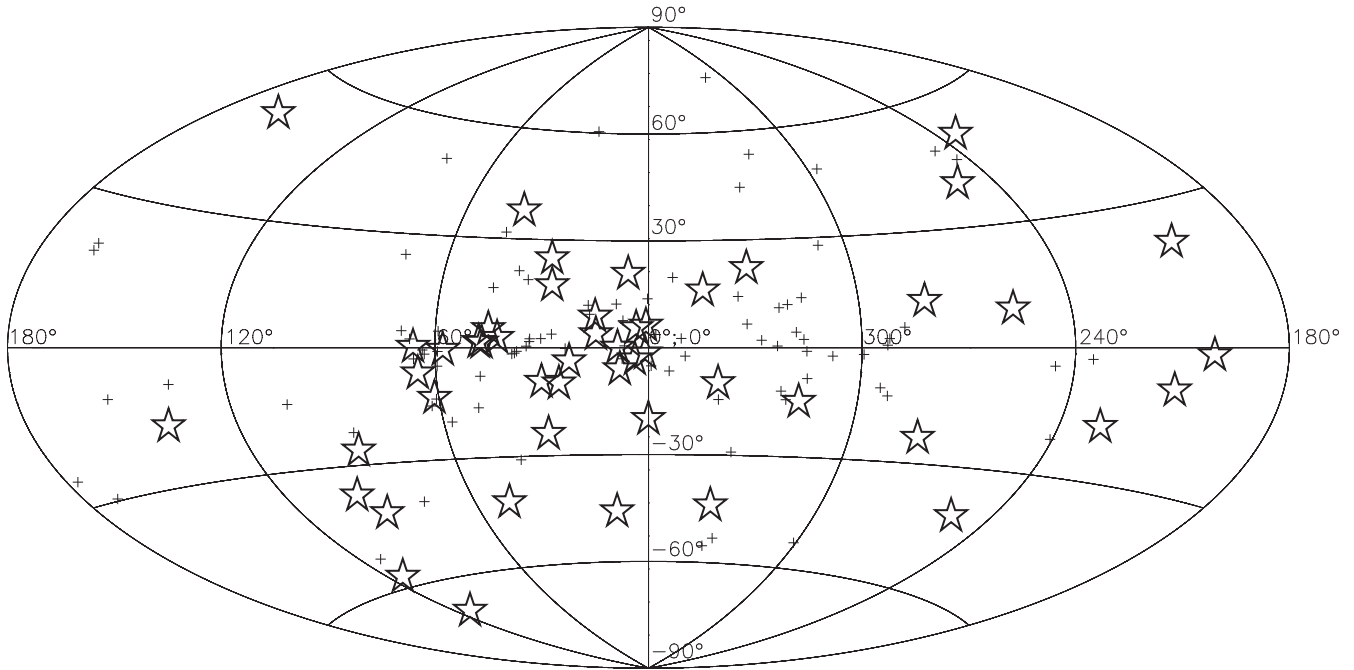
Figure 1. Plot of the Galactic distribution of all presently known Galactic-disc MSPs (as found in the ATNF pulsar catalogue version 1.51; Manchester et al. 2005). MSPs currently part of the IPTA are indicated by star symbols, all other Galactic MSPs that are detected in radio and do not inhabit globular clusters, are indicated by crosses. Galactic latitude is on the vertical axis; Galactic longitude on the horizontal axis, increasing leftward, with the Galactic Centre at the origin. Several newly discovered pulsars that are presently being evaluated in terms of potential timing precision, fill holes in the current PTA distribution, particularly at high Northern latitudes and in the Galactic anticentre.

To correctly and straightforwardly perform the steps listed above in future IPTA efforts, we therefore discuss the complications and shortcomings of current PTA data sets and provide recommendations that will facilitate IPTA research in the future. Specifically, we briefly describe the current state of the IPTA and its technical set-up in Section 2; list specifics of the data sets currently available and discuss the practical difficulties inherent to this present data set in Section 3. Since the current state of IPTA data combination leaves much to be desired (a situation we attempt to remedy in this work), the data set presented here is relatively outdated and therefore not optimally sensitive to GWs. Nevertheless, to illustrate the difference the IPTA can provide, we present limits on the strength of a GWB, both for the individual PTA data sets and the combined data set, in Section 4. As the goal of our work is to ease PTA research in the future, we present a summary of challenges and expected progress beyond this work, on both technical and analytic fronts, in Section 5; and Section 6 concludes the paper with a list of projects based on combined IPTA data sets. A detailed list of recommendations for pulsar timing projects is presented in Appendix A, where we propose a 'best practice' for pulsar timing formats and methods.

2 THE IPTA

The IPTA consists of three regional PTAs: the EPTA, NANOGrav and the PPTA, as listed in Table 1. These three arrays are complementary in their capabilities, most specifically in their sky coverage and in their observing frequencies, which are crucial for correction of time-variable interstellar effects, as described in more detail in Section 3.1. Furthermore, the combined data from these three PTAs can increase the average observing cadence by a factor of up to 6, further improving the sensitivity to GWs.

2.1 The IPTA source list

The combined source list of the current IPTA data release contains 49 MSPs, of which 14 are solitary and 35 are in binary orbits. The binary MSPs are mostly orbited by helium white dwarfs (28 systems), with six CO white-dwarf binaries and one black-widow system (PSR J1610−2100). The global placement of our telescopes allows IPTA pulsars to be spread across the entire sky, as shown in Fig. 1. Because the known MSP population is concentrated in the Galactic disc and in the inner Galaxy, the IPTA sources also cluster in those regions. (Note this clustering is not necessarily physical, but partly a consequence of the inhomogeneous surveying performed so far.) In the search for isotropic stochastic correlated signals, the sky position of pulsars is not in itself of importance, but the distribution of angular separations between pulsar pairs does impact the sensitivity (Hellings & Downs 1983).[6] Fig. 2 shows the histogram of the angular separations in the IPTA sample and Table 3 shows the pairs of pulsars with the largest and smallest angular distances on the sky. Clearly small angles, up to ∼70° are most densely sampled, but the angular sampling is overall quite uniform, notwithstanding the apparent clustering of our pulsars towards the inner Galaxy. An important point of note, however, is that for many practical purposes only a subset of these 49 pulsars may be used. Specifically, only a handful of these pulsars dominate constraints on GWs, which is primarily a consequence of the wide range in timing precision obtained on these sources, something that is not taken into account in the theoretical analyses mentioned in Section 1.3 but which has been considered in the context of observing schedule optimization (Lee et al. 2012).

---

[6] Note that for anisotropic searches, the absolute sky positions do matter.
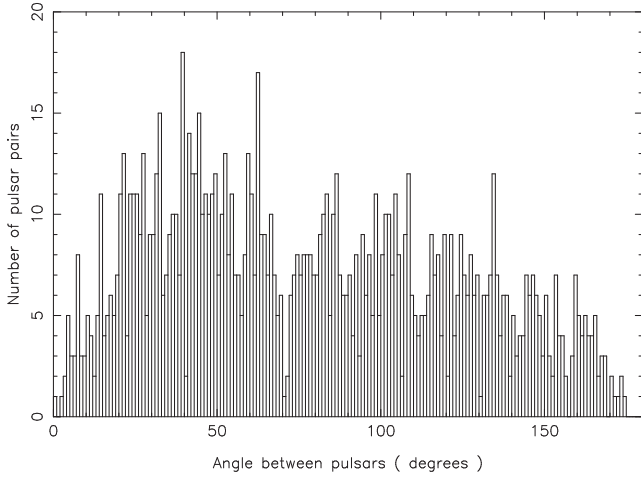
Figure 2. Histogram of the angular separation between the IPTA pulsars. Even though the pulsars are not spread out evenly on the sky (see Fig. 1), the angular separation between pulsars has a relatively uniform coverage. In this histogram, every bin corresponds to 1°.

Table 3. Pulsar pairs with the largest and smallest angular separations on the sky.

Pulsar name (J2000)	Pulsar name (J2000)	Angular separation (°)
J1910+1256	J1911+1347	0.88
J1721−2457	J1730−2304	2.79
J1751−2857	J1804−2717	3.32
J1853+1303	J1857+0943	3.47
J1853+1303	J1910+1256	4.14
J0621+1002	J1843−1113	174.5
J0621+1002	J1801−1417	173.5
J0751+1807	J2010−1323	173.4
J1012+5307	J2129−5721	172.6
J0613−0200	J1738+0333	171.1

As can be seen in Fig. 3, recent surveys have resulted in a very strong growth of the known MSP population. Before these new MSPs can be usefully employed in PTA analyses, however, their timing models must be adequately determined and their timing precision needs to be evaluated. For these reasons (and the strong dependence of GW sensitivity on the timing baseline, as discussed in Section 1.3), the current data set is dominated by MSPs discovered in the mid-1990s and early 2000s. Many more MSPs are already being monitored by the various PTAs, but these are not effective for GW detection efforts yet and are excluded from this work. Some preliminary results on those new discoveries were recently presented by Arzoumanian et al. (2015) and included in the IPTA source list of Manchester & IPTA (2013). The complete list of MSPs contained in the first IPTA data release, is given in Table 2, along with some basic characteristics.

2.2 Constituent data sets

As listed in Table 1, the IPTA data set is a combination of the data sets presented by the three PTAs independently: the NANOGrav 5-yr data set (Demorest et al. 2013), spanning from 2005 to 2010; the extended PPTA Data Release 1 (Manchester et al. 2013), ranging from 1996 to 2011 February; and the EPTA Data Release
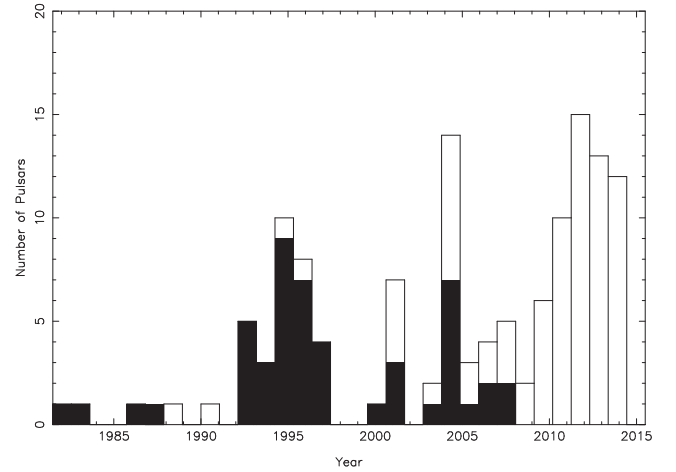
Figure 3. Histogram showing the discovery dates of all known MSPs belonging to the Galactic disc population (as featured in the ATNF pulsar catalogue; Manchester et al. 2005). The MSPs contained in the current IPTA data set are indicated in black. Multiple new discoveries are not included in this first IPTA data combination as the constituent data sets are slightly aged and the timing baselines for most recently discovered pulsars were too short to significantly add to PTA work at the time, but more recently many of these sources have been included in PTAs, e.g. by Arzoumanian et al. (2015) and these sources will be contained in future IPTA work.

1.0 (Desvignes et al. 2016), covering 1996 to mid-2014; complemented by the publicly available data from Kaspi et al. (1994) on PSRs J1857+0943 and J1939+2134 (timed from their discoveries in 1982 and 1984, respectively, until the end of 1992) and the extended NANOGrav data on PSR J1713+0747 (Zhu et al. 2015, extended from its discovery in 1992 to the end of 2013).[7] These data sets typically average observations in both frequency and time, leading to a single ToA per pulsar, observation and telescope. There are three exceptions to this: the Demorest et al. (2013) NANOGrav data are timed without frequency averaging, so each frequency-channel provides a single ToA; the Zhu et al. (2015) data were partially averaged in time (up to 30 min) and frequency (final frequency resolution dependent on the observing frequency and instrument used); and observations made with the Parkes dual 10/50-cm receiver result in two ToAs: one per observing band.

Two differences exist between the data presented here and those published by the individual PTAs. The PPTA data differ for PSR J1909−3744 as the initial version published by Manchester et al. (2013) had instrumental offsets fixed at values that were suboptimal for this high-precision data set. The updated PSR J1909−3744 data used in our analysis have these offsets determined from the data and have been extended with more recent observations; this version of the PPTA data is described in more detail by Shannon et al. (2015). The EPTA data differ as the data set described by Desvignes et al. (2016) contains additional digital-filterbank data for several pulsars. This subset of the EPTA data does add some more ToAs, though their precision is limited given the low sensitivity of the instrument. This limits the contribution to the IPTA data set as a whole, justifying its exclusion from our analysis.

Finally, to ensure consistency between pulsars and improve the analysis, all timing models made use of the DE421 Solar-system ephemeris model (Folkner, Williams & Boggs 2009), used a

---

[7] The analysis of further archival data from the Arecibo telescope is ongoing and will likely further extend the baseline and increase the cadence for other pulsars too; but inclusion of these data is left for a future paper.

solar-wind density model with a density of four electrons per cubic cm at 1 au (You et al. 2007b) and were referred to the TT(BIPM2013) time-scale using barycentric coordinate time (TCB Hobbs, Edwards & Manchester 2006).

3 CREATING THE IPTA DATA SET

In the analysis of long, high-precision pulsar timing data sets, four fundamental challenges arise.

First, delays in or changes to observing hardware cause time offsets between different telescopes and observing systems, which are derived from the data through fitting of arbitrary offsets (so-called 'jumps') between systems, which can lower the sensitivity to signals of interest.

Secondly, imperfections in the data analysis and relevant algorithms as well as possible environmental and elevation-dependent effects, conspire with noise and noise-like artefacts in the observations to corrupt the estimation of ToA uncertainties. This is particularly a problem for pulsars that scintillate strongly. Scintillation is a propagation effect caused by the ionized interstellar medium (IISM) and to first-order results in order-of-magnitude variations in the observed flux density of a pulsar, making the ToA uncertainty highly variable, too. The strength of scintillation depends strongly on the observing frequency, distance to the pulsar and the nature of the IISM between us and the pulsar in question. For a more complete overview of scintillation (and some of its higher order effects), the interested reader is referred to Rickett (1990) and Stinebring (2013).

For sources that do not show significant scintillation this problem is limited, since uncertainties could simply be ignored without much loss of information; but since the IPTA MSP sample consists of mostly nearby sources (see Table 2), scintillation does occur,[8] especially for the brightest and most precisely timed MSPs. Ignoring the ToA uncertainties thereby worsens timing precision (i.e. the rms of the data set and its sensitivity to timing parameters) dramatically, implying that a more accurate estimate of the timing uncertainties is needed. This problem is compounded by the large variation in the types of calibration that have been applied to the data. Because pulsar emission is typically highly polarized, imperfections in the receiver systems can cause corruptions to the pulse shape if the systems are not properly calibrated for polarization (Sandhu et al. 1997; van Straten 2013). These effects are strongly receiver and telescope dependent and so are not equally important for each data set. Furthermore, the different levels at which the IPTA data have been calibrated imply that any calibration-related imperfections will affect different subsets quite differently, thereby adding importance to the underestimation of ToA uncertainties.

Thirdly, because pulsars are high-velocity objects, the lines of sight to them move slightly through the Galaxy during our observing campaign. This combines with small-scale structures in the IISM and results in time-variable, frequency-dependent variations in ToAs. These variations may be accounted for in the pulsar timing model, provided multifrequency data are available at all times; alternatively a mathematical description needs to be used to interpolate between (or extrapolate from) multifrequency epochs.

The fourth and final challenge for long-term, high-precision pulsar timing is low-frequency noise. This does not directly affect the precision of the ToAs themselves, but can significantly distort the timing model and complicates combination of data sets that are not (fully) overlapping in time. Low-frequency noise could have instrumental origins (which can be correlated between pulsars; van Straten 2013) or might be intrinsic to the pulsar, as is the case for slow pulsars (Hobbs, Lyne & Kramer 2010b). This unexplained, long-term noise is of particular concern for PTAs as PTA projects are long-term projects by definition.

In this section, we first describe each of these issues in detail, along with the approach taken to measure and correct these in the IPTA data (Section 3.1). Subsequently, in Section 3.3, the results from our analysis are presented and any shortcomings of the present data set in this regard are identified. Many of these shortcomings could be avoided or limited in future (large-scale) pulsar timing projects, provided some 'rules of best practice' are followed. A list of such recommendations is presented in Appendix A.

3.1 Complications of IPTA data combination

Each of the IPTA's constituent data sets is highly inhomogeneous, combining a large number of different telescopes and/or data recording systems and observing frequencies. In addition to this, the observing cadence is often highly irregular and occasionally observations at a particular observatory or observing frequency are interrupted entirely for instrumental upgrades (see Fig. 4). For the longer data sets especially, observing set-ups (central observing frequencies, bandwidths, integration times and cadences) changed in time, making the statistical properties of these data sets highly non-stationary. These aspects greatly complicate any analysis and make the properties of the three PTA data sets very different. Consequently, each of the PTAs has developed its own tools and practices to correct the four main challenges listed earlier, but by design these approaches are often hard to extend to the data from the other collaborations. To best account for all described effects simultaneously, we chose to employ the recently developed TEMPONEST software (Lentati et al. 2014) in our analysis. TEMPONEST is an extension to the TEMPO2 software package (Hobbs et al. 2006) that performs the timing analysis within a Bayesian framework. Further details are given below and by Lentati et al. (2014).

3.1.1 Definition of systemic offsets

Time delays in the signal chain between the telescope's focus (where the pulsar signal is first received) and the hardware that applies a time stamp (which can be traced to a time standard) to the data, are supposedly constant in time, but can differ greatly between different observing systems and telescopes. Methods to measure these time offsets between different systems, at a level of precision beyond the presently achieved pulsar timing precision, are being developed (Manchester et al. 2013; Arzoumanian et al. 2015), but are as yet in their infancy and not widely adopted, or only applicable to data from multiple systems on a single telescope. Consequently, in combining heterogeneous data, all observing set-ups that could have different instrumental delays must be aligned by subtraction of a constant phase offset that is part of the timing model.[9]

To this end, homogeneous *systems* were identified within the data. A system in this context is defined as a unique combination of observing telescope, recording system and receiver (or centre

---

[8] Note that scintillation can combine with frequency-dependent variations in the pulse profile shape to cause systematic corruptions to ToAs. As discussed in Appendix A, approaches to prevent such corruptions have recently been developed.

[9] Assuming that offsets are within a pulse period; and that larger offsets have already been corrected.
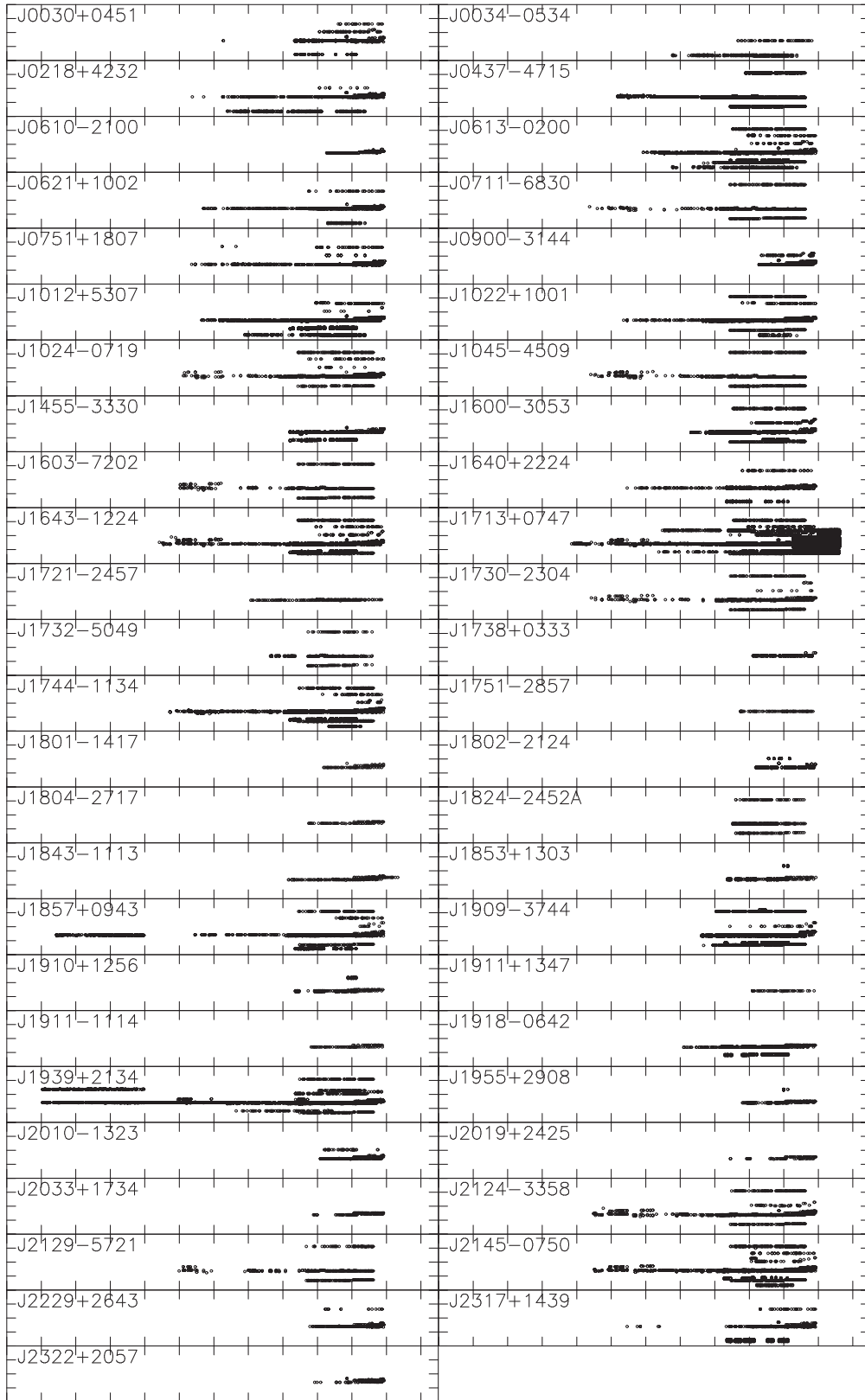
Figure 4. Plot of temporal and frequency coverage for all pulsars. The ranges of each subplot are identical and cover the MJD-range 45 000–57 500 (1982 January 31–2016 April 22) in X and 0–4 GHz in Y. Tick marks are at 1000-d and 1-GHz intervals. Note that only the centre frequency of each ToA is plotted (i.e. the bandwidth is ignored) and that many pulsars have only a few years of data at a single frequency.

frequency) used. For the EPTA telescopes, the receiver information was not always available, so if multiple receivers were used interchangeably at the same centre frequency (as is the case in particular for the Effelsberg 100-m radio telescope), this was ignored and both receivers were considered the same. In the case of historic PPTA data, a further complication arose since the earliest data were analysed by Verbiest et al. (2009), whereas more recent data (from the same observing systems) were analysed through independent pipelines, thereby introducing another arbitrary phase offset. In these cases, distinction was made between versions of the same system at different times. In some cases fewer than five ToAs were identified as a single system. Such systems (and their ToAs) were removed from the analysis as they add very little information, particularly after determining a systemic offset and uncertainty factors (see the next subsection).

Because Manchester et al. (2013) did determine some instrumental time delays at high precision, these PPTA systems were bound together in *groups* and offsets within such groups were not determined, except for PSRs J0437−4715, J1713+0747 and J1909−3744, which are more sensitive to these offsets than the independent measurements made by Manchester et al. (2013). Subsequently constant time offsets between all groups and ungrouped systems were determined. A discussion of the measured offsets (and mostly of the limitations of the available data sets in this regard) is given in Section 3.3 and suggested improvements for future work on this topic are listed in Appendix A.

3.1.2 Determining the measurement uncertainties

It has long been known that the uncertainties of ToAs do not accurately describe their scatter (Liu et al. 2011). There are two known reasons for this, though more unidentified reasons may exist. First, the standard approach to ToA determination proposed by Taylor (1992) does not determine the formal uncertainty on the ToAs, but instead calculates an approximate value that underestimates the true error in the low-S/N regime. Secondly, in the high-S/N regime, pulse-phase jitter (or SWIMS) will become relevant and add an extra noise component to the ToAs (see Section 1.1). The resulting underestimation of ToA uncertainties has a direct impact on the uncertainties of the timing model parameters. More importantly for the IPTA, if the underestimation is different for different telescopes or receiving systems, then different subsets will effectively be weighted more strongly than others, without actual justification.

Two standard statistical approaches can be used to amend this situation. First, ToA uncertainties can simply be multiplied by a system-dependent factor, the so-called 'error factor' or EFAC. This approach might be justified in case an S/N-dependent underestimation of the ToA uncertainty is present. Alternatively, uncertainties can be increased through quadrature addition of a constant noise level, the so-called 'quadrature-added error' or EQUAD. This approach is mostly justified in the high-S/N regime, where pulse-phase jitter adds a random variation to the ToAs, which is unquantified by the Gaussian noise in the off-pulse region of the observation (Osłowski et al. 2011), or in case a (possibly instrumental) noise floor exists (as e.g. shown in fig. 2 of Verbiest et al. 2010).

Historically, EQUADs have been applied before EFACs (Edwards et al. 2006):

$$\sigma_{\text{new}} = F\sqrt{Q^2 + \sigma_{\text{old}}^2}, \qquad (5)$$

where F and Q are the EFAC and EQUAD values, respectively. This may seem counter-intuitive given the physical reasoning laid

out above. The TEMPONEST software implements the application in reverse order, namely (Lentati et al. 2014):

$$\sigma_{\text{new}} = \sqrt{Q^2 + F^2\sigma_{\text{old}}^2}. \qquad (6)$$

In practice, both of these approaches are too simplified to be optimal (as discussed in detail by Shannon et al. 2014), since jitter noise (and therefore some part of the EQUAD) should decrease with the square root of the integration length and the mechanisms underlying the need for an EFAC are still relatively poorly quantified.

A third correction factor for ToA uncertainties is the 'error correction factor' or ECORR, introduced by Arzoumanian et al. (2014) and described in detail by van Haasteren & Vallisneri (2014). This factor accounts for pulse-phase jitter in two ways: it functions as an EQUAD factor in the determination of uncertainties; and it takes into consideration correlations between simultaneous ToAs taken at different observing frequencies. In particular for the NANOGrav data this factor is important, as the highly sensitive NANOGrav data are split in frequency bands that are narrower than the bandwidth of pulse-phase jitter, implying the jitter component is fully correlated between ToAs (Osłowski et al. 2011).

For the IPTA data combination, EFAC and EQUAD values were derived for all systems (as defined in Section 3.1.1) and ECORR values were determined for all NANOGrav systems. In doing so, we used the TEMPONEST definition of EQUAD and EFAC and will do so henceforth. Practically this makes no difference for the EFAC, but in the case of the EQUADs, the values that we report must be divided by the EFAC value in order to obtain the equivalent quantity according to the TEMPO2 definition.

3.1.3 Modelling interstellar dispersion variability

Because of dispersion in the IISM, radio signals undergo a frequency-dependent delay when traversing ionized clouds in our Galaxy (Lorimer & Kramer 2005):

$$t = D \times \frac{\text{DM}}{f^2}, \qquad (7)$$

with $D = 4.148\,808 \times 10^3\,\text{MHz}^2\,\text{cm}^3\,\text{s}\,\text{pc}^{-1}$, f the observing frequency and the dispersion measure $\text{DM} = \int_0^d n_e(l)\,\text{d}l$ the integrated electron density between us and the pulsar along the line of sight. This effect in itself has little impact on high-precision timing, but because of the high spatial velocities of pulsars and because of the Earth's motion around the Sun, the lines of sight to our pulsars sample changing paths through density variations in the IISM, thereby making this delay time-variable. Such a time-variable signal clearly does affect pulsar timing efforts, especially on the longest time-scales, where both the IISM effects (Armstrong, Rickett & Spangler 1995) and the GWB (Sesana 2013) are strongest.[10]

Correcting these interstellar delays (henceforth referred to as 'DM variations') is not necessarily problematic, provided adequate multifrequency data are available at all times. In reality, however, multifrequency data are often intermittent or lacking altogether (as can be seen in Fig. 4), or are of insufficient quality. This has made corrections for DM variations a significant problem, which has been dealt with in a variety of ways in the past.

Traditionally, time-derivatives of DM were included in the timing model (e.g. by Cognard et al. 1995), but in case of sufficiently dense

---

[10] Note that, depending on the GW source population, it has been shown that the GWB may peak at higher frequencies, too (Sesana et al. 2004; Enoki & Nagashima 2007).

sampling, smoothed time series have also occasionally been applied (Kaspi et al. 1994). More recently such smoothing has been developed further (You et al. 2007a; Keith et al. 2013), but this approach only really works well if the multifrequency sampling is relatively homogeneous throughout the data set. Furthermore, the most recent of these developments (Keith et al. 2013) does not take into consideration the uncertainties of the individual DM measurements. The issue of DM correction becomes even more complex in highly sensitive wideband systems, where the frequency-dependence of the pulse profile shape introduces possible correlations with the measured DM (Liu et al. 2014; Pennucci, Demorest & Ransom 2014), causing Demorest et al. (2013) to propose a correction method specifically aimed at such data, but difficult to apply to less sensitive, more narrow-band observations.

TEMPONEST does not indirectly correct for DM variability, like most previous methods did, but directly implements a spectral model of the DM variations and obtains the posterior probability distribution for the model parameters that define its power spectrum, taking into account the entire data set rather than individual observing epochs one at a time. Specifically, for the IPTA data combination discussed here, two-parameter power-law models[11] with f^{-2} scaling were evaluated and included in the final timing models in case significant evidence for such variations existed. In addition to such a power-law model, an annual DM variation was evaluated for PSR J0613−0200, because Keith et al. (2013) identified such a trend; and individual DM 'events' (i.e. short-term changes that do not follow the power-law model but do have a f^{-2} behaviour) were evaluated for PSRs J1603−7202 and J1713+0747, in agreement with Keith et al. (2013) and Desvignes et al. (2016), respectively. Details of the DM event models are given by Lentati et al. (2016). Contrary to Keith et al. (2013), our analysis showed no evidence for annual DM variations in excess of our power-law model, for PSR J0613−0200. This is primarily caused by the fact that our power-law model already contains DM variations at the periodicity of a year, while the analysis by Keith et al. (2013) quantified the total power of DM variations on a yearly time-scale, rather than the excess DM variations beyond a power-law model.

3.1.4 Evaluation of intrinsic pulsar timing instabilities

A final difficulty in long-term, high-precision pulsar timing is the presence of intrinsic pulsar timing noise. Such long-period noise has long been documented in slow pulsars (e.g. Boynton et al. 1972) and a few exceptional MSPs also display this property (Kaspi et al. 1994), though most MSPs have to date shown surprising levels of stability (Verbiest et al. 2009; Manchester et al. 2013). As time spans become longer and instrumentation becomes more sensitive, however, instabilities and their associated low-frequency noise become clearer and start to affect subsequent pulsar analyses (Verbiest et al. 2008; Coles et al. 2011) and in particular the search for long-period GWs. This is particularly so if predictions of steep-spectrum timing noise in MSPs hold true (Shannon & Cordes 2010). In order to cope with this, as part of the data combination, individual low-frequency noise models that do not depend on the observing frequency were determined for each pulsar. Furthermore, in order to accommodate the possibility of instabilities in the observing

hardware, the presence of low-frequency noise in every observing system independently was investigated.

As for the DM modelling, we only consider power-law models and refer to Lentati et al. (2016) for a full comparison of spectral models. The results of our analysis are summarized in Section 3.3.

3.2 Determination of pulsar timing parameters

In addition to the group and system offsets, the EFACs and EQUADs, the DM spectra and low-frequency noise, all traditional parameters of the pulsar timing model such as pulse period and spin-down, astrometric position and proper motion, parallax (where detectable), dispersion measure and any orbital parameters, are jointly evaluated by TEMPONEST. Especially for binary pulsars, a wide variety of orbital parameters (and relativistic time-derivatives thereof) could be included in the timing model. Parameters that were not detected with at least 90 per cent confidence, were not included in the timing models. In some cases, apparently relativistic terms can have geometric causes (e.g. a binary pulsar with high proper motion could be observed to have an anomalous periastron advance; see Kopeikin 1995, 1996). We have not undertaken the interpretation of such terms and translation into geometric parameters (inclination, longitude of the ascending node) if this was not already done by the authors of the respective input data sets, as this does not affect our results and as this astrophysical interpretation of the timing signatures may decrease the stability of the pulsar timing fit (adding more timing parameters without additional information). In these cases, we have used whichever timing model parameters were used by the individual PTAs.

For all determined parameters, this analysis results in probability distributions obtained through marginalization over the entire parameter space. For the deterministic parameters (these are all the parameters except those quantifying the white noise, red noise and DM variations), this marginalization was done analytically, using the linearized timing model as already implemented in TEMPO2. For the stochastic parameters (i.e. the white noise, red noise and DM variations), the marginalization was done numerically. The results are discussed in the following section.

3.3 The combined data set: results

The combined data set is available in the additional online material and on the internet at http://www.ipta4gw.org. It is provided in three different forms.

(i) Combination 'A': a raw form that has jumps, but no EFACs, EQUADs, DM or red-noise models included.

(ii) Combination 'B': a default 'TEMPO2' form which includes jumps, EFACs, TEMPO2-format EQUADs (i.e. following equation 5), a DM model implemented through DM-offset flags ('-dmo') added to the ToA lines, a red-noise model in the form of a spectral model compatible with the Cholesky TEMPO2 code introduced by Coles et al. (2011), but no ECORRs.

(iii) Combination 'C': a TEMPONEST combination with JUMPS, EFAC, ECORRs, EQUADs (following equation 6) and DM and red noise models compatible with the TEMPONEST code.

The post-fit timing residuals with the maximum likelihood DM-variation signal subtracted are shown in Fig. 5. Red noise that was inconsistent with DM variations was assumed to be intrinsic in nature and was not subtracted. Some fundamental characteristics describing these post-fit data are summarized in Table 4. A brief summary of the results of our analysis along with some comments

---

[11] Note that the spectral shape is fundamentally free and that different spectral models can be evaluated. A complete comparison of the evidence for different DM spectral models will be presented in a paper by Lentati et al. (2016); here, we merely use the most likely model, which is a power law.
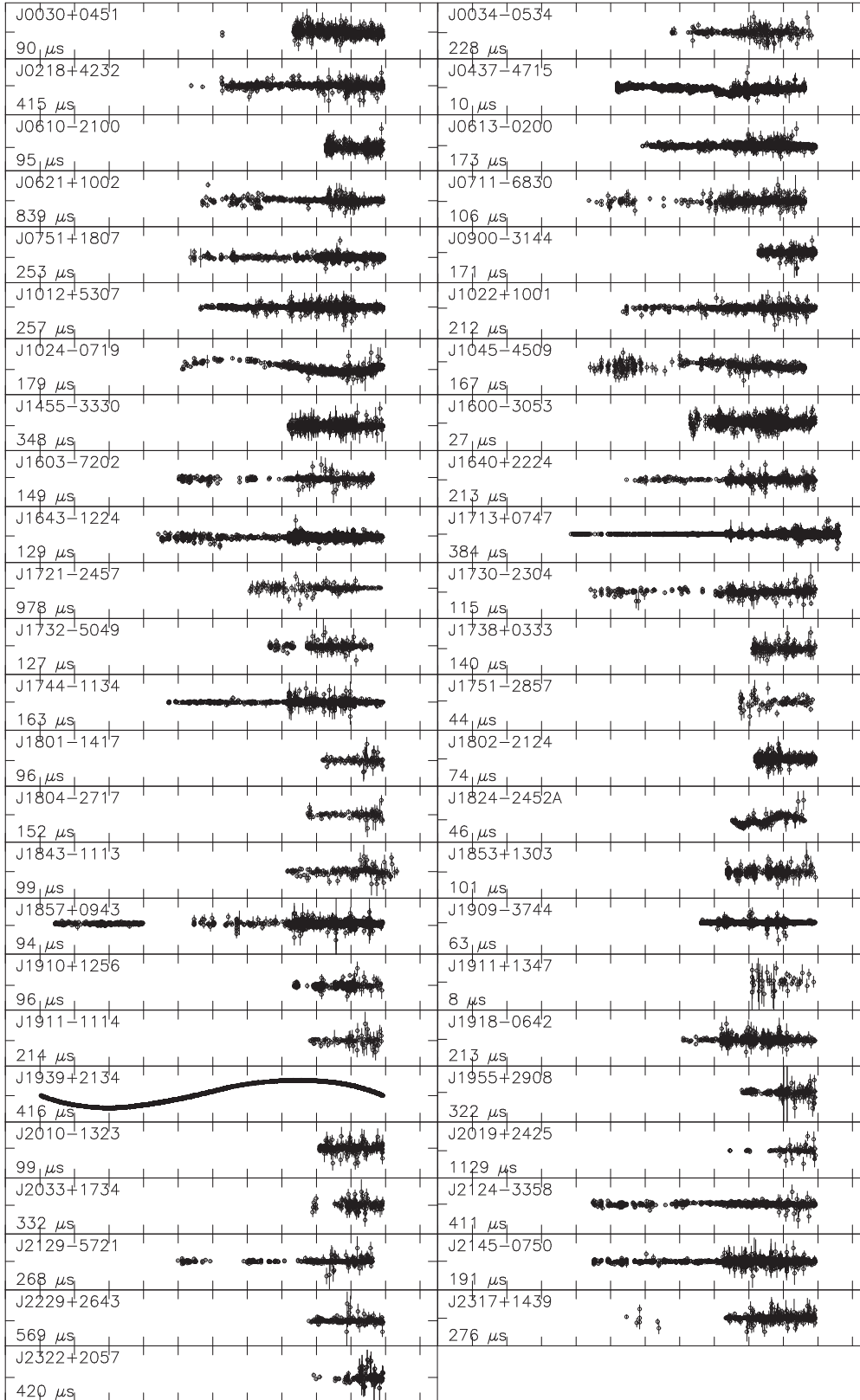
Figure 5. Plot of all timing residuals. Shown are the residuals (i.e. observed ToA minus model-predicted ToA) after subtraction of the DM model, but with inclusion of any modelled red noise. The X range is as in Fig. 4, covering the MJD range 45 000–57 500 (1982 31 January–2016 April 22) with tick marks at 1000-d intervals; the Y range is different for each pulsar: the numbers in the plot indicate the full plotted Y range for each pulsar.

Table 4. Summary table of the combined data set. The columns give, respectively, the pulsar name, the time span in years, the MJD range, the weighted rms of the timing residuals (after subtraction of the timing model and DM variations), the number of ToAs, the average time between days on which the pulsar is observed and the number of telescopes from which data were included in the current data set. The final two columns show whether DM variations or timing noise (i.e. long-period noise intrinsic to the pulsar) were detected ('y') or not ('n') in the data set. In cases where long-period noise was detected but no distinction could be made between DM or intrinsic noise, the label 'Undetermined' is used across both the 'DM variations' and 'Timing noise' columns. Five pulsars had linear or quadratic trends in DM that were formally significant at the 1σ level, but which were strongly correlated to the pulsar's spin period or period derivative. Those five pulsars are identified with 'Undetermined' only in the 'DM variations' column. For six pulsars system-dependent long-period noise was detected. These are marked as 's' in the 'Timing noise' column, as this system-dependent noise has the characteristics of timing noise, but is likely instrumental.

Pulsar name (J2000)	Time span (yr)	MJD range	Residual rms (μs)	Number of ToAs	Average cadence (d)	Number of telescopes	DM variations	Timing noise
J0030+0451	12.7	51275–55924	1.9	1250	6.6	3	Undetermined	
J0034−0534	11.1	51770–55808	4.4	267	24.0	2	y	n
J0218+4232	15.2	50370–55924	6.7	1005	7.6	4	y	n
J0437−4715	14.9	50190–55619	0.3	5052	5.1	1	y	s
J0610−2100	4.5	54270–55925	5.2	347	10.9	2	n	n
J0613−0200	13.7	50931–55926	1.2	2940	4.3	6	y	y
J0621+1002	14.3	50693–55921	11.5	637	10.6	4	y	y
J0711−6830	17.1	49373–55619	2.0	549	18.2	1	y	n
J0751+1807	15.3	50363–55948	3.5	1129	10.4	4	Undetermined	
J0900−3144	4.5	54284–55922	3.4	575	3.1	2	Undetermined	
J1012+5307	14.4	50647–55924	1.7	2910	6.3	5	y	y
J1022+1001	15.2	50361–55923	2.2	1375	6.5	5	y	s
J1024−0719	15.9	50117–55922	5.9	918	8.4	5	y	y
J1045−4509	17.0	49405–55619	3.3	635	16.9	1	y	n
J1455−3330	7.4	53217–55926	4.0	1495	5.9	3	y	s
J1600−3053	9.9	52301–55919	0.8	1697	5.1	4	y	s
J1603−7202	15.3	50026–55618	2.3	483	19.3	1	y	n
J1640+2224	15.0	50459–55924	2.0	1139	12.9	5	y	n
J1643−1224	17.8	49421–55919	2.7	2395	6.9	6	y	s
J1713+0747	21.2	48850–56598	0.3	19972	5.1	7	y	y
J1721−2457	10.3	52076–55853	25.5	152	24.9	2	n	n
J1730−2304	17.8	49421–55920	2.1	563	15.9	4	y	s
J1732−5049	8.0	52647–55582	2.5	242	18.8	1	y	n
J1738+0333	4.9	54103–55905	2.6	206	27.7	1	n	n
J1744−1134	17.0	49729–55925	1.1	2589	8.4	6	Undetermined	
J1751−2857	5.7	53746–55836	2.4	78	26.8	1	n	n
J1801−1417	4.8	54184–55920	4.6	86	20.2	2	Undetermined	
J1802−2124	4.7	54188–55916	4.3	433	24.8	2	Undetermined	
J1804−2717	5.9	53747–55914	4.5	76	28.9	2	Undetermined	n
J1824−2452A	5.8	53518–55619	2.4	298	13.6	1	y	y
J1843−1113	8.7	53156–56331	1.7	186	17.5	3	Undetermined	
J1853+1303	7.0	53370–55922	1.1	566	24.5	3	n	n
J1857+0943	26.0	46437–55916	1.3	1641	13.4	6	y	n
J1909−3744	10.8	53041–56980	0.2	2623	4.4	3	y	n
J1910+1256	6.9	53370–55886	3.0	597	25.2	3	Undetermined	
J1911+1347	4.9	54092–55868	0.6	45	40.4	1	Undetermined	n
J1911−1114	5.7	53815–55880	5.2	81	25.5	2	n	n
J1918−0642	10.5	52095–55914	1.5	1522	13.4	4	y	n
J1939+2134	27.1	46024–55924	70.0	3905	4.6	6	y	y
J1955+2908	5.8	53798–55918	5.0	319	16.6	3	n	n
J2010−1323	5.0	54086–55917	1.9	296	6.3	2	y	n
J2019+2425	6.8	53446–55920	8.8	80	31.7	2	Undetermined	n
J2033+1734	5.5	53894–55917	13.3	130	15.6	2	Undetermined	n
J2124−3358	17.6	49489–55924	3.0	1115	7.7	3	y	n
J2129−5721	15.4	49987–55618	1.2	447	19.2	1	y	n
J2145−0750	17.5	49517–55922	1.2	2347	7.0	6	y	y
J2229+2643	5.8	53790–55920	3.8	234	9.6	3	y	n
J2317+1439	14.9	50458–55917	1.6	867	13.5	5	y	n
J2322+2057	5.5	53916–55920	6.9	199	15.0	2	Undetermined	n

on the limitations and specificities of this data set and analysis are given below.

ToA Selection. In combining the IPTA data set, an attempt was made to limit the analysis to a simple combination of the data, without further selection. However, in a few cases ToAs that were included in existing data sets have been removed or flagged for future reference. Specifically, this includes the following three types of ToAs:

Simultaneous: ToAs that were observed at the same observatory with different instruments that operated at identical or (partially) overlapping frequency bands, have not been removed, but have been identified with '-simul' flags on their ToA lines. This is particularly relevant for 64 ToAs from the PSR J1713+0747 data set from Zhu et al. (2015), where during the years 1998–2004 the ABPP and Mark 4 recorders were used simultaneously at Arecibo (see Splaver et al. 2005, for more details).

Solar wind: when the line of sight to a pulsar comes close to the Sun, the increased electron density of the solar wind causes additional dispersive delays. Therefore, ToAs that are taken along lines of sight that are within $5°$ of the Sun have been commented out.[12] The $5°$ threshold is somewhat arbitrary but is a conservative value based on the model predictions presented by Ord, Johnston & Sarkissian (2007).

Small groups: systems with fewer than five ToAs have been removed from the analysis (see Section 3.1.1) as they increase the complexity by adding systemic offsets, but do not add sufficient information to reliably allow determination of their uncertainties (EFAC and EQUAD values). Such systems with few ToAs occur particularly in the PPTA data sets, which were originally analysed using a larger set of simultaneous ToAs that are no longer available. Since the IPTA data set improves the pulsar timing models, a renewed evaluation of systemic offsets and ToA uncertainties is in order, but cannot be performed on such limited systems without the inclusion of the simultaneous data (which were unavailable for this work).

Systemic offsets. In principle, the large number of pulsars and long overlapping time span of the data analysed should make it possible to identify instrumental offsets more precisely by averaging the offsets measured in different pulsars, as long as the differences in instrumental delays are within a pulse period. There are both practical and technical reasons why this does not work in the present data set.

Practically this can be done only if the reference phase used for timing is identical for all pulsars. This can be accomplished by phase-aligning the template profiles for the different systems through cross-correlation. While this has been done to some degree for each PTA separately, the phase-offsets between PTAs were not measured based on the template profiles – and in either case such information was unavailable for the historic data (sub)sets from Kaspi et al. (1994) and Verbiest et al. (2009). Technically this situation is complicated by the wide variety of recording systems. Various (mostly older) systems experience different time delays depending on the pulse period and DM of the pulsar being observed. In particular, differences between older systems where dedispersion may have been performed in hardware and newer systems where this is

done in software would produce variable time offsets for different pulsars. This makes the measurement of systemic offsets nearly intractable.

Measurement uncertainties. As introduced in Section 3.1.2, underestimated uncertainties on pulse ToAs are accounted for using uncertainty-multiplication factors (EFACs, F), uncertainties added in quadrature (EQUADs, Q) and additional correlated error factors (ECORRS). Physically the primary source of EQUADs and ECORRs is expected to be pulse-phase jitter noise (Shannon et al. 2014), while EFACs are most likely caused by imperfections in the algorithm chosen for the uncertainty determination (see Appendix A). As with systemic offsets, the size and variety of the combined IPTA data should allow a more detailed investigation of these factors. However, as with the systemic offsets, such an exercise is complicated by the many parameters that affect these values, as described below.

We find that for most pulsars, the F values derived for different observing systems follow a Gaussian distribution centred near unity, with a spread of the order of 0.3. The majority (57 per cent) of systems have Q values below 10 ns, indicating that little or no evidence exists for additional white noise. For the significant Q measurements, typical values were on the order of microseconds or less, with maximum Q values between 20 and 40 µs found for a few fainter pulsars at observing bands with less sensitivity. For 16 pulsars, two ECORR values were used (one per observing band) but for PSR J1713+0747 14 ECORR values were needed, given the large number of highly sensitive systems present in the Zhu et al. (2015) data set. The ECORR values were detected in the vast majority of these cases, with maxima around 3 µs and a median of 270 ns.

A few pulsars have wider distributions for their F values, for two possible reasons. First, pulsars like PSRs J1713+0747 and J1939+2134 have extended data sets with early data from old observing systems that are not present in the data sets from the other pulsars. Since the technical specifications of observing systems have dramatically improved over the past few decades, it should not be surprising that systematic effects linked to limited resolution and sensitivity led to lower quality data in the past, thereby causing less reliable ToA uncertainties. Therefore, data sets containing both recent and 20-yr old data are likely to have a wider spread for F. A second contributing factor is the possible correlation between F and potentially unquantified white noise, Q. Specifically for observing systems with only few ToAs and for weakly scintillating sources (i.e. if all ToAs have comparable measurement uncertainty), it is mathematically impossible to disentangle F from Q. In these cases, anomalously low values for F (of the order of 0.1) are possible in combination with comparably large values for Q (of the order of 10 µs or more).

Pulsars that show significant values for Q mostly do so for only a single or few observing systems (and typically not the most sensitive systems), indicating that these significant values for Q are fundamentally artefacts of correlations in the analysis (e.g. correlations between F and Q as described above). A few of the brightest pulsars, including PSR J1909−3744, show significant values for Q for many observing systems. For PSR J1909−3744 this result stands in sharp contrast to the more advanced research of Shannon et al. (2014), who found the pulse-phase jitter noise in this pulsar to be limited to 10 ns or less (in hour-long observations). This again indicates our poor understanding of the systematics that cause ToA uncertainties to be underestimated and requires further investigations, which go beyond the capabilities of our data.

In summary, a large majority of the pulsars observed did not require significant EFAC, EQUAD or ECORR values. In the pulsars

---

[12] These ToAs are undesirable for most experiments, but might be used to investigate solar-wind effects. Hence, they were not deleted from the data set, but inserted as comments in the data files, thereby excluding them from any standard analysis whilst keeping them available for potential solar-wind investigations.

with the longest timing baselines, a clear improvement has been observed with lower F and Q values for more recent observing systems. Some pulsars, however, require inexplicably high values (for Q in particular), well in excess of independently measured bounds on pulse-phase jitter. These pulsars warrant more detailed investigation as an unknown noise source appears to be contributing to their timing.

DM variability and timing instabilities. As described earlier, DM variations typically have a long-term character, similar to intrinsic instabilities in pulsar timing (known as 'timing noise'). Given the poor multifrequency sampling on many of our sources (see Fig. 4), it is in many cases impossible to distinguish these two types of variations; even when multiple frequencies are present, the possible mismatch in the timing precision at these frequencies can make measurements of DM variability in these data imprecise and highly covariant with timing noise estimates. Consequently, the analysis of these two sources of long-period noise is closely intertwined and complex and will not be discussed in detail here, but referred to a companion paper (Lentati et al. 2016). However below, we briefly summarize and comment on the main findings of this research.

As listed in Table 4, 17 of the 49 pulsars in the IPTA data set do not show evidence of excess low-frequency noise (i.e. show neither DM variations nor timing instabilities). This is to be expected if the data set in question is relatively short, as is the case for all but one of these pulsars, which have data lengths of less than 15 yr. The remaining source, PSR J2124−3358, has a data set of 17.6 yr with a residual rms of 3.8 µs and is therefore highly sensitive to low-frequency noise, so its absence indicates that this pulsar is inherently a very stable rotator.

Eight pulsars in our sample have evidence of both DM variability and timing instabilities. Not surprisingly, this group contains the pulsars with the longest time spans: PSRs J1939+2134 (27.1 yr) and J1713+0747 (21.2 yr). Another eight pulsars show evidence for low-frequency noise, but have no sufficiently sensitive multifrequency data; therefore, no distinction can be made between intrinsic pulsar timing noise and DM variations. (Even though the data sets on PSRs J0030+0451, J0751+1807, J0900−3144 and J1744−1134 contain ToAs at multiple frequencies, the measurement precision and cadence turn out to be insufficient in these cases.) 15 pulsars show significant DM variations but no frequency-independent timing noise.

A particularly powerful aspect of the combined IPTA data set is that the timing instabilities of different telescopes and observing systems can be checked against each other, thereby clarifying whether the observed timing noise is caused by hardware issues, or whether it is truly intrinsic to the pulsar. Such a test was already performed on a smaller scale by van Haasteren et al. (2011), who found that for the few pulsars and telescopes they compared, low-frequency noise models were consistent. A similar analysis based on the IPTA data set presented here, also mostly finds consistent models, except for six pulsars that show system-dependent low-frequency noise in addition to DM variations. In some cases this system-dependent noise is not simply dependent on the observing hardware, but on the frequency band in which the observations were taken, suggesting a possible interstellar origin other than dispersion. For the full analysis, we refer to Lentati et al. (2016).

In summary, of the 26 pulsars with more than a decade of data, a vast majority (25 pulsars) show (possible) DM variations and just over a third (10 pulsars) show (possible) system-independent timing noise. Only one of these 26 pulsars (PSR J1721−2457) shows no evidence for DM variations or red noise at all, but the timing of this pulsar has been exclusively undertaken at a single frequency, so that

any long-term DM variations would most likely be absorbed in fits for pulse period and period derivative.

4 LIMITS ON THE GWB AMPLITUDE

As discussed in detail above, the present data set is a useful testbed for general IPTA-like data combination efforts. While this combination was ongoing, however, individual PTAs have been updating their data sets more rapidly and have meanwhile improved their sensitivity, particularly to the GWB, which is telescope-independent (unlike instrumental effects) and highly sensitive to the length of the data set. A full, detailed analysis of the present IPTA data set with regards to obtaining a limit on the strength of the GWB is therefore not worthwhile at present. Instead, we present a simplified analysis on both the combined and the constituent data sets, to illustrate the potential impact an IPTA combination can provide, as this is analytically intractable. Based on the work presented elsewhere in this paper, combination of IPTA data will in the future become more straightforward, allowing a shorter timeline and therefore more significant GWB limits to be derived using IPTA data.

To derive an indicative limit on the GWB amplitude, we used the PICCARD software package.[13] This code has been cross-checked with TEMPONEST (Lentati et al. 2014) and uses the same likelihood functions. The noise model used is as described elsewhere in this paper, i.e. including EFAC, EQUAD and ECORR values to properly quantify the white noise, but with a more general red-noise model that allowed the power spectral density amplitudes to vary per frequency bin and did not implicitly assume a power-law shape. This deviation from the more extensive noise models presented by Lentati et al. (2016) was made in order to avoid a full re-analysis of the Lentati et al. (2016) work including GW limits. For the scope of this paper, an indicative bound that could be compared between the different data sets, was sought rather than an exhaustive GW-limit analysis. A combined GW-limit analysis with full noise modelling is beyond the scope of this paper and is deferred to a future and more competitive IPTA data release. The sampling was done with the Gibbs sampler introduced by van Haasteren & Vallisneri (2014). To reduce computing time and avoid complications caused by some less precisely timed pulsars, only the four pulsars with the highest sensitivity (as quantified through the length of their data set and the precision and number of their ToAs) were included in this analysis. These are PSRs J0437−4715, J1713+0747, J1744−1134 and J1909−3744. Furthermore, correlations of the GWB signal between pulsars have been neglected and no advanced noise-modelling (as in Lentati et al. 2016) was performed, i.e. no system-specific red noise was included. Even though the individual PTAs have previously published limits based on the constituent data sets, we perform our analysis again on the individual PTA data sets, because the published limits were derived using slightly different noise models than ours, so the limits cannot be directly and self-consistently compared to our IPTA-based limit. Efforts to find a more appropriate noise model are an ongoing effort within the IPTA (see e.g. Lentati et al. 2016).

Our results are summarized in Table 5. For the individual PTAs our limits are consistent with or slightly worse than those published by the individual PTAs, which is expected given the fact that our analysis is more basic and less detailed than those published elsewhere. In the case of NANOGrav, the limit we calculate is better than the one published by Demorest et al. (2013) because of the

---

[13] https://github.com/vhaasteren/piccard

Table 5. Limits on the GWB from the combined IPTA data set and its PTA-specific subsets. Given are the data set for which the limit was determined, the limit on the GWB amplitude resulting from our basic analysis; and the limit published based on the same subsets (with any differences described in Section 2.2), along with their bibliographic reference. Note our limits are generally slightly worse because of the basic nature of our analysis, with the exception of the NANOGrav data set, as this one was significantly extended by including the PSR J1713+0747 data from Zhu et al. (2015).

PTA subset	GWB limit ($\times 10^{-15}$)	Published limit ($\times 10^{-15}$)	Reference
NANOGrav	4.5	1.5	Arzoumanian et al. (2016)
EPTA	3.3	3.0	Lentati et al. (2015)
PPTA	2.8	1.0	Shannon et al. (2015)
IPTA	1.7		

inclusion of the long data set of PSR J1713+0747 by Zhu et al. (2015). For the PPTA data set, our limit is less constraining than their most recent limit, but we use all data available on the pulsars used, including lower frequency ToAs that are affected by more severe (and not well modelled) low-frequency noise; furthermore, the recent limit by Shannon et al. (2015) extended the timing baseline with high-quality data, further improving the overall timing precision. As expected, the IPTA limit beats the lowest limit by an individual PTA, by as much as a factor of 1.6. While this is a basic analysis that lacks the rigour of a full investigation, it can be expected that future IPTA work would also improve limits on the GWB amplitude by a similar factor. More importantly, though, since the IPTA contains a larger number of pulsars than any of the constituent PTAs (a logical consequence of the complete sky coverage) and given the strong scaling of PTA sensitivity with the number of pulsars (equations 3 and 4), it is clear that the IPTA has a unique advantage when it comes to carrying out the first actual detection of GWs with pulsar-timing data.

5 THE FUTURE OF THE IPTA

The present IPTA data combination is a relatively ad hoc combination of (largely archival) timing data from a variety of observing projects. It uses a large number of (mostly old) instruments and focuses on a relatively poorly defined set of MSPs that has been discovered in the course of the past few decades. In Section 1, we have described how the pulsar timing sensitivity depends on the telescope's sensitivity and how the sensitivity of PTAs depends on the pulsars in their sample. All of these aspects are about to go through a revolution and in a few years time the updated IPTA data set will greatly differ from the present one and will likely be sensitive to GWB with amplitudes far below 1×10^{-15}. In the following, we briefly describe the main progress that can be expected for the coming decade, above and beyond the addition of more recent data. This includes some technical advances to the pulsar timing methodology (Section 5.1), which are being developed now and should bear fruit soon, the potential expansion of the pulsar sample (Section 5.2) and the impact significantly more sensitive telescopes could make (Section 5.3) over the course of coming decades.

5.1 Beating systematics

Several aspects of pulsar timing require further research and development in order to improve data quality and long-term data usefulness. Some straightforward practical measures have been laid out in

Appendix A, but several more fundamental questions remain to be solved in the coming few years, in preparation for the leap in sensitivity the Square Kilometre Array (SKA) will bring. Specifically, we identify four main aspects of ongoing study of key relevance to PTA research.

DM-correction methods. As described in Section 3.1.3, correction methods for temporal DM variations have essentially always been ad hoc, based on whatever (limited) data were available and without a thorough understanding of the processes that underly these variations. The analysis presented in this paper is no exception to this rule.

Early work by Foster & Cordes (1990) found that in order to correct DM variations in pulsar timing data, regular multifrequency observations with less-sensitive telescopes would be more efficient in mitigating the variable IISM effects than less regular but more sensitive observations. However, with increased telescope sensitivity and bandwidths since then, new questions have arisen. Most importantly, because of the different refraction angles at the different frequencies, the IISM sampled by observations at different wavelengths might differ slightly (Cordes, Shannon & Stinebring 2016). It is yet unknown whether the magnitude of this effect is relevant for the observations included in the IPTA, but for the new generation of low-frequency telescopes this question is key to evaluating their usefulness for PTA-type work. Initial work on a limited set of slow pulsars by Hassall et al. (2012) found that no such 'frequency-dependent DM' could be identified, but this test needs to be reproduced for the lines of sight to the MSPs in the IPTA sample.

A second unknown on this topic is whether a single, ultrawide observing bandwidth (including potential issues with radio frequency interference (RFI) and system temperature) would be preferred to a set of simultaneous observations at various, widely separated observing frequencies; or whether a fully independent observing campaign at ultralow frequencies with high cadence (e.g. as aperture arrays could provide through multibeaming) would be more sensitive and therefore more beneficial. This likely depends on the RFI environment and on the spectral index of the pulsar as well as its pulse-shape evolution with frequency and may therefore require a sizeable study to achieve clarity.

Finally, DM correction methods either interpolate or smooth the measured DM values (You et al. 2007a; Keith et al. 2013); or assume a model that is fitted to them (Cognard et al. 1995; Lentati et al. 2014). However, these approaches inherently assume the DM variations are time-stationary with the exception of a limited number of top-hat-like 'events', but this is demonstrably *not* the case (see e.g. Maitia, Lestrade & Cognard 2003; Coles et al. 2015). As our sensitivity improves with lower frequency telescopes, wider bandwidths and longer data sets, the characterization of the IISM's numerous effects should improve. This would increase our understanding of the IISM and should allow more accurate DM correction methods.

Also, as bandwidths increase and future generations of telescopes become more sensitive, direct in-band DM determination as part of the timing model, without interpolation or model assumptions (as already proposed by Demorest et al. 2013), may become more widely applicable.

Higher-order IISM effects. In addition to changes in dispersion, density variations in the IISM can cause temporal variations in scattering and thereby change the pulse shape as a function of time (Hemberger & Stinebring 2008). While this effect is mostly undetectable at observing frequencies of a GHz or higher with present telescopes, its amplitude is mostly unknown and this may

Table 6. List of major ongoing pulsar surveys. Given are the survey acronym, telescope used, centre frequency, starting year and literature reference.

Survey acronym	Telescope used	Frequency (MHz)	Start year	Reference
PALFA	AO	1400	2004	Cordes et al. (2006)
GBNCC	GBT	350	2009	Stovall et al. (2014)
Fermi PSC	Various	Various	2009	Ray et al. (2012)
AO327	AO	327	2010	Deneva et al. (2013)
HTRU-S	PKS	1352	2008	Keith et al. (2010)
HTRU-N	EFF	1360	2010	Barr et al. (2013)
LOTAAS	LOFAR	135	2014	Coenen et al. (2014)

affect more sensitive observations with upcoming telescopes like the Five-hundred-metre Aperture Spherical radio Telescope (FAST) or the SKA. Detailed experiments with mitigation methods such as cyclic spectroscopy (Demorest 2011, as performed at lower frequencies by Walker, Demorest & van Straten 2013; Archibald et al. 2014) are therefore required on a larger sample of MSPs, particularly because any newly discovered pulsars are likely to be fainter and therefore more distant than the currently known population, making scattering effects more likely to have a significant impact.

Absolute system offsets. In principle, systemic offsets can be determined with high precision using interferometric fringe-fitting on baseband data, at least for the most recent generation of digital recorders. Such efforts are ongoing (Dolch et al. 2014; Bassa et al. 2016). An alternative method that has recently been developed, is based on correlating the identical noise in the data from two data recorders on the same telescope, as introduced by Arzoumanian et al. (2015) in their appendix A. This last technique could also be used on multitelescope data (as a form of intensity interferometry), but is likely to give less precise results than the actual interferometric efforts mentioned before.

Improved calibration. In cases where the observations are correctly polarization-calibrated, the timing precision of some pulsars may be significantly enhanced by using the polarimetric information in the pulse profile (van Straten 2006). While this method is promising and has been used with good results already (van Straten 2013), its application is still non-standard and somewhat marginal in the current IPTA data set. This is likely because of the difficulty in reliably modelling any impurities in the receiver system; and time-variations thereof (see e.g. van Straten 2013). Proper characterization and monitoring of receiver properties could therefore provide further enhancements to pulsar timing precision. Especially at lower observing frequencies and with highly sensitive, future telescopes, frequency and time-dependent changes in the polarimetric position angle of the pulsar radiation, as most significantly introduced by time-variable Faraday rotation in the ionosphere (Sotomayor-Beltran et al. 2013), may also need to be corrected for, which is not typically the case presently. (Note that ionospheric RM variation measurements may be a side-product of advanced calibration techniques, as shown in fig. 8 of Osłowski et al. 2013.)

Advanced white-noise modelling. As discussed in Appendix A, EFAC, EQUAD and ECORR determination methods should be more extensive, to take into account certain expected scaling relations (e.g. $Q \propto T^{-1/2}$). However, all of the effects listed above also add impurities to the timing residuals, which are not necessarily reflected in the ToA uncertainties. It is therefore safer to measure the effect of phenomena like pulse-phase jitter on the ToA uncertainty directly (as recently done by Shannon et al. 2014, for the PPTA pul-

sars), rather than to implement EQUAD measurement methods that assume jitter as the key contributor. Such a bottom-up approach also ensures the correct interpretation of ToA uncertainty underestimation and thereby removes any possible but unphysical correlations that might exist. A first step in that direction is the determination of ECORR values, which by design quantify the EQUAD part that correlates between simultaneous ToAs and as such already move towards a more physical understanding of these ad hoc parameters.

SWIMS mitigation. As described in Section 1.1, two noise sources affect pulsar timing data: radiometer noise and pulse-phase jitter or SWIMS (Osłowski et al. 2011). The former of these can only be reduced through hardware upgrades, the impact of the latter can be reduced through generalized least-squares template-matching techniques, like those proposed by Osłowski et al. (2011). Such techniques not have been fully developed yet, but in the coming era of highly sensitive radio telescopes this may well become a fundamental tool of radio pulsar timing. For practical applications, Osłowski et al. (2011, 2013) did propose a mitigation method that can presently be applied to pulsar timing work.

5.2 Pulsar surveys

Pulsar surveys are long-term undertakings as both observing and processing requirements are extremely large. As a list of the most prominent on-going pulsar surveys shows (Table 6), many of the world's major radio telescopes are currently – and have been for multiple years – involved in surveys for pulsars. This concerted effort has led to an MSP discovery rate that is unprecedented (see Fig. 3) and even though none of these recently discovered MSPs have made it into the first IPTA data release, the monitoring and evaluation of these sources for IPTA use is ongoing and is already lengthening the source lists of individual PTAs (see e.g. Arzoumanian et al. 2015). This is particularly important given the strong scaling of PTA sensitivity with the number of pulsars (see equations 3 and 4).

For the IPTA, there are three prime reasons to support ongoing pulsar surveys. First, the larger the number of pulsars in the IPTA, the more sensitivity the IPTA has to any correlated signal. While this is technically true (see the equations in Section 1.3), it depends strongly on the *timeability* of the pulsars in question, i.e. mostly on their flux density and pulse width (or the integrated derivative of the pulse profile, to be precise), as shown in equation (1). So while fainter, slower MSPs can still be useful for the IPTA, they will be useful only if the observing time dedicated to them is proportionally increased (Lee et al. 2012). This means that the required observing time may become prohibitively large. A second advantage, however, is that existing pulsars in the array may be replaced by new

discoveries. This is particularly relevant since the strength of timing noise differs greatly from pulsar to pulsar (see Fig. 5), so that for long-term projects the stability of the pulsar will become more important than its instantaneous timing precision. A third and final benefit of ongoing pulsar surveys is their use for PTA experiments with the next generation of radio telescopes (see Section 5.3). As telescope sensitivity increases, the radiometer noise will decrease and a far larger set of pulsars will become useful (Liu et al. 2011).

5.3 SKA and pathfinder telescopes

In the coming decade, the construction and use of the SKA will commence and, with its order-of-magnitude increase in sensitivity, it will revolutionize all aspects of the science discussed in this paper. Specifically, pulsar surveys with the SKA (Keane et al. 2015) will multiply the number of pulsars available for PTA research; and PTA sensitivity based on both newly discovered and already known pulsars will not merely enable GW detection, but likely commence the field of low-frequency GW astronomy (Janssen et al. 2015). In anticipation of these events, a host of 'pathfinder' telescopes are currently being constructed, commissioned and used, paving the way towards the SKA revolution in a wide range of aspects.

Low-frequency pathfinders. Three low-frequency SKA pathfinders are currently operational for pulsar research. These are the European LOw-Frequency ARray (LOFAR; Stappers et al. 2011; van Haarlem et al. 2013), the Long-Wavelength Array (LWA) in New Mexico (Dowell et al. 2013) and the Murchison Widefield Array (MWA; Bhat et al. 2014) in Western Australia. Since the Galactic synchrotron background emission has a steeper spectral index than the typical pulsar (Bates, Lorimer & Verbiest 2013), these low-frequency arrays are not optimal for highly sensitive timing efforts, but given the strong frequency dependence of interstellar effects (see equation 7 and further effects in Lorimer & Kramer 2005), these pathfinders could prove to be highly useful tools for monitoring and correcting variability in the IISM (Kondratiev et al. 2016).

FAST and LEAP. FAST is an Arecibo-type spherical telescope currently being constructed in China; and will be the world's largest and most sensitive single-dish radio telescope upon completion. Its receiver platform is also moveable so that a substantial part of the sky can be observed (Nan et al. 2011). Another sensitive project is the Large European Array for Pulsars (LEAP; Bassa et al. 2016), which coherently combines the data from the five major centimetre-wavelength radio telescopes in Europe, thereby synthesizing an Arecibo-sized telescope that is able to point in any direction of the Northern sky. With its unrivalled instantaneous sensitivity, FAST should be able to make a major contribution to pulsar surveys (Yue, Li & Nan 2013), particularly if equipped with a multibeam receiver of phased-array feed, since the limited beamwidth will either necessitate vast amounts of observing time to complete a survey of any part of the sky; or require the survey to be undertaken at lower frequencies. More importantly, the increased sensitivity of these telescopes will allow improved timing precision which will enhance the sensitivity of PTAs to GWs (and other signals) to levels beyond the reach of current technology (Zhao et al. 2013).

MeerKAT. The MeerKAT telescope (Booth & Jonas 2012) is the South-African SKA pathfinder, located in the Karoo desert where the core of the mid- and high-frequency parts of the SKA will be located. MeerKAT will be more sensitive than the 100-m-class telescopes of the Northern hemisphere and up to five times more sensitive than Parkes, making it the most sensitive fully steerable

telescope in the world, placed in the Southern hemisphere, where many of the most precisely timed MSPs reside (Table 2). This will make it an important addition to PTA efforts in the lead up to the SKA.

6 CONCLUSIONS

In this paper, we present the creation of the first IPTA data release by combining the data from the three constituent PTAs and illustrate the importance of this for limits on GWB by comparing straightforward results from the subsets and the combined set. This indicates an IPTA combined limit on the GWB should be close to twice as sensitive as any of the constituent data sets. Further analyses of these data, particularly relating to the timing stability of MSPs (Lentati et al. 2016), Solar-system ephemeris and clock errors, will be published separately in due course. Beyond these specific projects, though, this work can be seen as a primer, identifying pitfalls and challenges with the formats and practices common in pulsar timing today. Through this first analysis, we hope the quality and ease of use of pulsar timing data can be vastly improved upon, so that subsequent IPTA analyses will be performed in a more rigorous manner, thereby preparing the field for both the advent of GW astronomy and the SKA era.

REFERENCES

Abdo A. A. et al., 2009, ApJ, 699, 1171
Abdo A. A. et al., 2010, ApJ, 712, 957
Archibald A. M., Kondratiev V. I., Hessels J. W. T., Stinebring D. R., 2014, ApJ, 790, L22
Armstrong J. W., Rickett B. J., Spangler S. R., 1995, ApJ, 443, 209
Arzoumanian Z., Brazier A., Burke-Spolaor S., Chamberlin S. J., Chatterjee S., Cordes J. M., Demorest P. B., Deng X., 2014, ApJ, 794, 141
Arzoumanian Z. et al., 2015, ApJ, 813, 65
Arzoumanian Z. et al., 2016, ApJ, preprint (arXiv:1602.05570)
Babak S. et al., 2015, MNRAS, 455, 1665
Backer D. C., Kulkarni S. R., Heiles C., Davis M. M., Goss W. M., 1982, Nature, 300, 615
Bailes M. et al., 1994, ApJ, 425, L41
Bailes M. et al., 1997, ApJ, 481, 386
Barr E. D. et al., 2013, MNRAS, 435, 2234
Bassa C. G. et al., 2016, MNRAS, 456, 2196
Bates S. D., Lorimer D. R., Verbiest J. P. W., 2013, MNRAS, 431, 1352
Bhat N. D. R. et al., 2014, ApJ, 791, L32
Booth R. S., Jonas J. L., 2012, Afr. Skies, 16, 101
Boriakoff V., Buccheri R., Fauci F., 1983, Nature, 304, 417
Boyle L. A., Buonanno A., 2008, Phys. Rev. D, 78, 043531
Boynton P. E., Groth E. J., Hutchinson D. P., Nanos G. P., Partridge R. B., Wilkinson D. T., 1972, ApJ, 175, 217
Burgay M. et al., 2006, MNRAS, 368, 283
Camilo F., 1995, PhD thesis, Princeton University
Camilo F., Nice D. J., Taylor J. H., 1993, ApJ, 412, L37

Camilo F., Nice D. J., Taylor J. H., 1996a, ApJ, 461, 812
Camilo F., Nice D. J., Shrauner J. A., Taylor J. H., 1996b, ApJ, 469, 819
Champion D. J. et al., 2010, ApJ, 720, L201
Coenen T. et al., 2014, A&A, 570, A60
Cognard I., Bourgois G., Lestrade J. F., Biraud F., Aubry D., Darchy B., Drouhin J. P., 1995, A&A, 296, 169
Coles W., Hobbs G., Champion D. J., Manchester R. N., Verbiest J. P. W., 2011, MNRAS, 418, 561
Coles W. A. et al., 2015, ApJ, 808, 113
Cordes J. M., Lazio T. J. W., 2002, preprint (astro-ph/0207156)
Cordes J. M. et al., 2006, ApJ, 637, 446
Cordes J. M., Shannon R. M., Stinebring D. R., 2016, ApJ, 817, 16
Damour T., Vilenkin A., 2000, Phys. Rev. Lett., 85, 3761
Deller A. T., Verbiest J. P. W., Tingay S. J., Bailes M., 2008, ApJ, 685, L67
Demorest P. B., 2011, MNRAS, 416, 2821
Demorest P. B. et al., 2013, ApJ, 762, 94
Deneva J. S., Stovall K., McLaughlin M. A., Bates S. D., Freire P. C. C., Martinez J. G., Jenet F., Bagchi M., 2013, ApJ, 775, 51
Desvignes G. et al., 2016, MNRAS, submitted (arXiv:1602.08511)
Dolch T. et al., 2014, ApJ, 794, 21
Dowell J. et al., 2013, ApJ, 775, L28
Du Y., Yang J., Campbell R. M., Janssen G., Stappers B., Chen D., 2014, ApJ, 782, L38
Edwards R. T., Bailes M., 2001, ApJ, 553, 801
Edwards R. T., Hobbs G. B., Manchester R. N., 2006, MNRAS, 372, 1549
Enoki M., Nagashima M., 2007, Prog. Theor. Phys., 117, 241
Faulkner A. J. et al., 2004, MNRAS, 355, 147
Favata M., 2009, ApJ, 696, L159
Ferdman R. D. et al., 2010, ApJ, 711, 764
Finn L. S., Lommen A. N., 2010, ApJ, 718, 1400
Folkner W. M., Williams J. G., Boggs D. H., 2009, in Pollara F., ed., The Interplanetary Network (IPN) Progress Report, The Planetary and Lunar Ephemeris DE 421. Jet Propulsion Laboratory, p. 42
Foster R. S., Backer D. C., 1990, ApJ, 361, 300
Foster R. S., Cordes J. M., 1990, ApJ, 364, 123
Foster R. S., Wolszczan A., Camilo F., 1993, ApJ, 410, L91
Frail D. A., Weisberg J. M., 1990, AJ, 100, 743
Freire P. C. C. et al., 2012, MNRAS, 423, 3328
Gonzalez M. E. et al., 2011, ApJ, 743, 102
Grishchuk L. P., 2005, Phys. Usp., 48, 1235
Hassall T. E. et al., 2012, A&A, 543, A66
Hellings R. W., Downs G. S., 1983, ApJ, 265, L39
Hemberger D. A., Stinebring D. R., 2008, ApJ, 674, L37
Hobbs G. et al., 2004a, MNRAS, 352, 1439
Hobbs G., Lyne A. G., Kramer M., Martin C. E., Jordan C., 2004b, MNRAS, 353, 1311
Hobbs G. B., Edwards R. T., Manchester R. N., 2006, MNRAS, 369, 655
Hobbs G. et al., 2010a, Class. Quantum Grav., 27, 084013
Hobbs G., Lyne A. G., Kramer M., 2010b, MNRAS, 402, 1027
Hobbs G. et al., 2012, MNRAS, 427, 2780
Hotan A. W., van Straten W., Manchester R. N., 2004, PASA, 21, 302
Hotan A. W., Bailes M., Ord S. M., 2006, MNRAS, 369, 1502
Jacoby B. A., 2004, PhD thesis, California Institute of Technology
Jacoby B. A., Bailes M., van Kerkwijk M. H., Ord S., Hotan A., Kulkarni S. R., Anderson S. B., 2003, ApJ, 599, L99
Jacoby B. A., Bailes M., Ord S. M., Knight H. S., Hotan A. W., 2007, ApJ, 656, 408
Janssen G. H., Stappers B. W., Bassa C. G., Cognard I., Kramer M., Theureau G., 2010, A&A, 514, A74
Janssen G. et al., 2015, in Bourke et al., eds, Proc. Sci, Advancing Astrophysics with the Square Kilometre Array (AASKA14). SISSA, Treiste, p. 37
Jenet F. A., Hobbs G. B., Lee K. J., Manchester R. N., 2005, ApJ, 625, L123
Johnston S. et al., 1993, Nature, 361, 613
Kaspi V. M., Taylor J. H., Ryba M., 1994, ApJ, 428, 713
Keane E. F. et al., 2015, in Bourke et al., eds, Proc. Sci, Advancing Astrophysics with the Square Kilometre Array (AASKA14). SISSA, Treiste, p. 40

Keith M. J. et al., 2010, MNRAS, 409, 619

Keith M. J. et al., 2013, MNRAS, 429, 2161

Khmelnitsky A., Rubakov V., 2014, J. Cosmol. Astropart. Phys., 2, 19

Kondratiev V. I. et al., 2016, A&A, 585, A128

Kopeikin S. M., 1995, ApJ, 439, L5

Kopeikin S. M., 1996, ApJ, 467, L93

Kramer M., Xilouris K. M., Lorimer D. R., Doroshenko O., Jessner A., Wielebinski R., Wolszczan A., Camilo F., 1998, ApJ, 501, 270

Lazaridis K. et al., 2009, MNRAS, 400, 805

Lee K. J., Wex N., Kramer M., Stappers B. W., Bassa C. G., Janssen G. H., Karuppusamy R., Smits R., 2011, MNRAS, 414, 3251

Lee K. J., Bassa C. G., Janssen G. H., Karuppusamy R., Kramer M., Smits R., Stappers B. W., 2012, MNRAS, 423, 2642

Lentati L., Alexander P., Hobson M. P., Feroz F., van Haasteren R., Lee K. J., Shannon R. M., 2014, MNRAS, 437, 3004

Lentati L. et al., 2015, MNRAS, 453, 2576

Lentati L. et al., 2016, preprint (arXiv:1602.05570)

Liu K., Verbiest J. P. W., Kramer M., Stappers B. W., van Straten W., Cordes J. M., 2011, MNRAS, 417, 2916

Liu K., Keane E. F., Lee K. J., Kramer M., Cordes J. M., Purver M. B., 2012, MNRAS, 420, 361

Liu K. et al., 2014, MNRAS, 443, 3752

Lommen A. N., Zepka A., Backer D. C., McLaughlin M., Cordes J. M., Arzoumanian Z., Xilouris K., 2000, ApJ, 545, 1007

Lommen A. N., Kipphorn R. A., Nice D. J., Splaver E. M., Stairs I. H., Backer D. C., 2006, ApJ, 642, 1012

Lorimer D. R., Kramer M., 2005, Handbook of Pulsar Astronomy. Cambridge Univ. Press, Cambridge

Lorimer D. R. et al., 1995, ApJ, 439, 933

Lorimer D. R., Lyne A. G., Bailes M., Manchester R. N., D'Amico N., Stappers B. W., Johnston S., Camilo F., 1996, MNRAS, 283, 1383

Lorimer D. R. et al., 2006, MNRAS, 372, 777

Lundgren S. C., Zepka A. F., Cordes J. M., 1995, ApJ, 453, 419

Lyne A. G., Brinklow A., Middleditch J., Kulkarni S. R., Backer D. C., Clifton T. R., 1987, Nature, 328, 399

Löhmer O., Lewandowski W., Wolszczan A., Wielebinski R., 2005, ApJ, 621, 388

Maitia V., Lestrade J.-F., Cognard I., 2003, ApJ, 582, 972

Manchester R. N., Hobbs G. B., Teoh A., Hobbs M., 2005, AJ, 129, 1993

IPTAManchester R. N., 2013, Class. Quantum Grav., 30, 224010

Manchester R. N., Hobbs G., Bailes M., Coles W. A., van Straten W., Keith M. J., 2013, Publ. Astron. Soc. Aust., 30, 17

Nan R. et al., 2011, Int. J. Mod. Phys. D, 20, 989

Navarro J., de Bruyn G., Frail D., Kulkarni S. R., Lyne A. G., 1995, ApJ, 455, L55

Nicastro L., Lyne A. G., Lorimer D. R., Harrison P. A., Bailes M., Skidmore B. D., 1995, MNRAS, 273, L68

Nice D. J., Taylor J. H., 1995, ApJ, 441, 429

Nice D. J., Taylor J. H., Fruchter A. S., 1993, ApJ, 402, L49

Nice D. J., Splaver E. M., Stairs I. H., 2001, ApJ, 549, 516

Nice D. J., Splaver E. M., Stairs I. H., Löhmer O., Jessner A., Kramer M., Cordes J. M., 2005, ApJ, 634, 1242

Ord S. M., Johnston S., Sarkissian J., 2007, Sol. Phys., 245, 109

Osłowski S., van Straten W., Hobbs G. B., Bailes M., Demorest P., 2011, MNRAS, 418, 1258

Osłowski S., van Straten W., Demorest P., Bailes M., 2013, MNRAS, 430, 416

Pennucci T. T., Demorest P. B., Ransom S. M., 2014, ApJ, 790, 93

Porayko N. K., Postnov K. A., 2014, Phys. Rev. D, 90, 062008

Pshirkov M. S., Baskaran D., Postnov K. A., 2010, MNRAS, 402, 417

Rajagopal M., Romani R. W., 1995, ApJ, 446, 543

Ray P. S., Thorsett S. E., Jenet F. A., van Kerkwijk M. H., Kulkarni S. R., Prince T. A., Sandhu J. S., Nice D. J., 1996, ApJ, 470, 1103

Ray P. S. et al., 2012, preprint (arXiv:1205.3089)

Rickett B. J., 1990, ARA&A, 28, 561

Romani R. W., 1989, in Ögelman H., van den Heuvel E. P. J., eds, Timing Neutron Stars Timing a Millisecond Pulsar Array. Kluwer, Dordrecht, p. 113

Rosado P. A., Sesana A., Gair J., 2015, MNRAS, 451, 2417

Sandhu J. S., Bailes M., Manchester R. N., Navarro J., Kulkarni S. R., Anderson S. B., 1997, ApJ, 478, L95

Sanidas S. A., Battye R. A., Stappers B. W., 2012, Phys. Rev. D, 85, 122003

Schwaller P., 2015, Phys. Rev. Lett., 115, 181101

Segelstein D. J., Rawley L. A., Stinebring D. R., Fruchter A. S., Taylor J. H., 1986, Nature, 322, 714

Sesana A., 2013, MNRAS, 433, L1

Sesana A., Haardt F., Madau P., Volonteri M., 2004, ApJ, 611, 623

Sesana A., Vecchio A., Volonteri M., 2009, MNRAS, 394, 2255

Seto N., 2009, MNRAS, 400, L38

Shannon R. M., Cordes J. M., 2010, ApJ, 725, 1607

Shannon R. M. et al., 2014, MNRAS, 443, 1463

Shannon R. M. et al., 2015, Science, 349, 1522

Siemens X., Ellis J., Jenet F., Romano J. D., 2013, Class. Quantum Grav., 30, 224015

Sotomayor-Beltran C. et al., 2013, A&A, 552, A58

Splaver E. M., 2004, PhD thesis, Princeton University

Splaver E. M., Nice D. J., Arzoumanian Z., Camilo F., Lyne A. G., Stairs I. H., 2002, ApJ, 581, 509

Splaver E. M., Nice D. J., Stairs I. H., Lommen A. N., Backer D. C., 2005, ApJ, 620, 405

Stairs I. H. et al., 2005, ApJ, 632, 1060

Stappers B. W., Hessels J. W. T., Alexov A., Anderson K., Coenen T., 2011, A&A, 530, A80

Stinebring D., 2013, Class. Quantum Grav., 30, 224006

Stovall K. et al., 2014, ApJ, 791, 67

Taylor J. H., 1992, Phil. Trans. R. Soc. A, 341, 117

Taylor S. R. et al., 2015, Phys. Rev. Lett., 115, 041101

Tiburzi C. et al., 2016, MNRAS, 455, 4339

Toscano M., Bailes M., Manchester R., Sandhu J., 1998, ApJ, 506, 863

Toscano M., Sandhu J. S., Bailes M., Manchester R. N., Britton M. C., Kulkarni S. R., Anderson S. B., Stappers B. W., 1999, MNRAS, 307, 925

van Haarlem M. P. et al., 2013, A&A, 556, A2

van Haasteren R., Levin Y., 2010, MNRAS, 401, 2372

van Haasteren R., Vallisneri M., 2014, Phys. Rev. D, 90, 104012

van Haasteren R., Levin Y., Janssen G. H., Lazaridis K., Kramer M., 2011, MNRAS, 414, 3117

van Straten W., 2006, ApJ, 642, 1004

van Straten W., 2013, ApJS, 204, 13

Verbiest J. P. W., Lorimer D. R., 2014, MNRAS, 444, 1859

Verbiest J. P. W. et al., 2008, ApJ, 679, 675

Verbiest J. P. W. et al., 2009, MNRAS, 400, 951

Verbiest J. P. W., Bailes M., Bhat N. D. R., Burke-Spolaor S., Champion D. J., 2010, Class. Quantum Grav., 27, 084015

Verbiest J. P. W., Weisberg J. M., Chael A. A., Lee K. J., Lorimer D. R., 2012, ApJ, 755, 39

Walker M. A., Demorest P. B., van Straten W., 2013, ApJ, 779, 99

Wang J. B. et al., 2015, MNRAS, 446, 1657

Wolszczan A. et al., 2000, ApJ, 528, 907

You X.-P. et al., 2007a, MNRAS, 378, 493

You X. P., Hobbs G. B., Coles W. A., Manchester R. N., Han J. L., 2007b, ApJ, 671, 907

Yue Y., Li D., Nan R., 2013, in van Leeuwen J., ed., Proc. IAU Symp. 291, Neutron Stars and Pulsars: Challenges and Opportunities after 80 years. Cambridge Univ. Press, Cambridge, p. 577

Zhao W., Zhang Y., You X.-P., Zhu Z.-H., 2013, Phys. Rev. D, 87, 124012

Zhu X.-J. et al., 2014, MNRAS, 444, 3709

Zhu W. W. et al., 2015, ApJ, 809, 41

APPENDIX A: THE IPTA TIMING FORMAT

Because of the unprecedented size, diversity and precision of the IPTA data set, the shortcomings of present pulsar timing practices have come out very clearly during this combination. We therefore present a series of guidelines detailing 'good pulsar timing practice', aimed at streamlining and optimizing future pulsar timing efforts, below.

Systemic offsets. As described earlier, the determination of systemic offsets between different telescopes and recording systems, is difficult. However, with an increased homogeneity in data recording systems (presently most pulsar data are created in software-based coherent-dedispersion systems), systemic offsets may become far more tractable. In order to ensure more accurate determination of these offsets in the future as well as to ensure the usefulness of present data sets for future use, we propose the following pulsar timing standard practices.

(i) When combining multiple systems, the reference system should be chosen as that system with the lowest value for $\sigma/\sqrt{N}$, where σ is the median ToA uncertainty for the system and N is the number of ToAs for this system in the data set. Since any offsets are measured with respect to the reference system, choosing a system with worse precision or fewer ToAs will increase the uncertainty of all measured systemic offsets.

(ii) Systemic offsets are part of the timing solution and are therefore stored as part of the pulsar timing model. To ease combination and for increased clarity and convenience, we recommend that for the reference system an unfitted offset with zero value is also included in the timing model.

(iii) Since absolute alignment of data sets can be assured only by cross-correlation of the standard templates used for creating these data sets, any ToAs should be accompanied by the template profile used to create them.

(iv) In cases where simultaneous ToAs are used to determine systemic offsets, all simultaneous ToAs should be contained in the released data. To properly weight these correlated ToAs, ideally information on their simultaneity would be included in a covariance matrix, though this is not effectively implemented as yet in the TEMPO2 software.

(v) Offsets between systems should never be absorbed in the ToAs. This is to avoid corruptions of the most basic measurement data (i.e. the ToAs) and to provide transparency and clarity.

Measurement uncertainties. The causes behind underestimation of ToA uncertainties are not fully clear yet, but a few aspects are understood and should be accounted for in pulsar timing investigations. In particular, we therefore suggest the following.

(i) For observations of scintillating pulsars across a bandwidth that is large enough to encompass significant frequency-dependent variations in the profile shape, biases to the ToAs would be introduced by variations in the brightness distribution across the observing band. This problem can be averted by reducing the frequency range per ToA (as done for the NANOGrav data), or by using frequency-dependent template profiles. This latter method has been simultaneously and independently implemented by two groups: Pennucci et al. (2014) and Liu et al. (2014).

(ii) The Fourier phase gradient method for ToA determination as proposed by Taylor (1992) measures the ToA of an observation by performing a phase-gradient fit to the Fourier transform of the cross-correlation of the observation and template profile. This traditional approach derives the ToA uncertainty from the second derivative of the χ^2 at the best-fitting point, like any standard χ^2 optimization routine. An alternative approach is to derive the uncertainty from a simple one-dimensional Markov-Chain Monte Carlo based on the likelihood as a function of phase-shift. In the PSRCHIVE software package (Hotan, van Straten & Manchester 2004), this method is implemented as '-A FDM' and should be the default ToA determination method. While the differences are negligible for high-S/N data, the standard χ^2 fit tends to underestimate ToA uncertainties

for low-S/N data (see Liu et al. 2011 and Arzoumanian et al. 2015, appendix B) so in these cases the FDM method is clearly preferred.

(iii) While often ignored, the additive white noise caused by pulse-phase jitter scales with the square-root of the number of pulses averaged. In order to create more reliable measurement uncertainties (and lower any EQUAD values), this jitter noise should be included in the timing analysis, which requires *the integration time* related to the ToAs.

This information, along with other descriptors of individual ToAs (such as bandwidth, number of time bins and number of frequency channels, all of which can affect the sensitivity of the system and therefore the uncertainties) needs to be stored as part of the raw data. To this end, the PSRCHIVE package has recently implemented the so-called 'IPTA' ToA format, which extends the ToAs with such meta-data.

(iv) To quantitatively assess outlier ToAs, a goodness-of-fit value (describing the template-to-observation fit) could be added to the metadata provided along with the ToAs. In PSRCHIVE, this option already exists in combination with the FDM method described above (and other methods such as MTM) and can be invoked through '-c gof'.

Dispersion measurements. As pulsar timing data sets become longer and more precise, they become even more sensitive to long-term DM variations. This means that multifrequency observing is crucial in the long-term, even for pulsars in which DM variations are yet to be observed. The optimal way of measuring and correcting variable DMs is still unclear, so the principal aim in pulsar timing should be to provide the basic multifrequency ToAs; and not derived DM values or models.

Intrinsic pulsar timing instabilities. Long-period variations seen in some MSPs are mostly consistent between telescopes (Lentati et al. 2016), indicating they are true astrophysical signals. However, some observing systems have been shown to be unreliable, producing signals which mimic intrinsic pulsar timing instabilities. Such unreliability can only be identified and remedied when comparable data sets from other telescopes exist.

[1]*Fakultät für Physik, Universität Bielefeld, Postfach 100131, D-33501 Bielefeld, Germany*

[2]*Max-Planck-Institut für Radioastronomie, Auf dem Hügel 69, D-53121 Bonn, Germany*

[3]*Astrophysics Group, Cavendish Laboratory, JJ Thomson Avenue, Cambridge CB3 0HE, UK*

[4]*CSIRO Astronomy and Space Science, Australia Telescope National Facility, PO Box 76, Epping, NSW 1710, Australia*

[5]*Jet Propulsion Laboratory, California Institute of Technology, 4800 Oak Grove Dr, M/S 67-201, Pasadena, CA 91109, USA*

[6]*National Radio Astronomy Observatory, PO Box O, Socorro, NM 87801, USA*

[7]*ASTRON, the Netherlands Institute for Radio Astronomy, Postbus 2, NL-7990 AA, Dwingeloo, the Netherlands*

[8]*Xinjiang Astronomical Observatory, Chinese Academy of Sciences, 150 Science 1-Street, Urumqi, Xinjiang 830011, China*

[9]*Jodrell Bank Centre for Astrophysics, School of Physics and Astronomy, The University of Manchester, Manchester M13 9PL, UK*

[10]*Center for Research and Exploration in Space Science and Technology/USRA and X-Ray Astrophysics Laboratory, NASA Goddard Space Flight Center, Code 662, Greenbelt, MD 20771, USA*

[11]*MPI for Gravitational Physics (Albert Einstein Institute), D-14476 Golm-Potsdam, Germany*

[12]*International Centre for Radio Astronomy Research, Curtin University, Bentley, WA 6102, Australia*

[13]*Cornell Center for Advanced Computing, Cornell University, Ithaca, NY 14853, USA*

[14]*Cornell Center for Astrophysics and Planetary Science, Cornell University, Ithaca, NY 14853, USA*

[15]*INAF-Osservatorio Astronomico di Cagliari, via della Scienza 5, I-09047 Selargius (CA), Italy*

[16]*Department of Physics, The Pennsylvania State University, University Park, PA 16802, USA*

[17]*Astronomy Department, Cornell University, Ithaca, NY 14853, USA*

[18]*Notre Dame of Maryland University, 4701 N. Charles Street, Baltimore, MD 21210, USA*

[19]*Laboratoire de Physique et Chimie de l'Environnement et de l'Espace LPC2E CNRS-Université d'Orléans, F-45071 Orléans, France*

[20]*Station de radioastronomie de Nançay, Observatoire de Paris, CNRS/INSU, F-18330 Nançay, France*

[21]*Department of Astronomy, School of Physics, Peking University, Beijing 100871, China*

[22]*Department of Physics, Hillsdale College, 33 E. College Street, Hillsdale, MI 49242, USA*

[23]*Department of Physics, Rutherford Physics Building, McGill University, 3600 University Street, Montreal, QC H3A 2T8, Canada*

[24]*Department of Physics and Astronomy, University of British Columbia, 6224 Agricultural Road, Vancouver, BC V6T 1Z1, Canada*

[25]*School of Mathematics, King's Buildings, University of Edinburgh, Edinburgh EH9 3JZ, UK*

[26]*Department of Physics and Astronomy, West Virginia University, Morgantown, WV 26506, USA*

[27]*Vancouver Coastal Health, Department of Nuclear Medicine, 899 W 12th Ae, Vancouver, BC V5Z 1M9, Canada*

[28]*Anton Pannekoek Institute for Astronomy, University of Amsterdam, Science Park 904, NL-1098 XH Amsterdam, the Netherlands*

[29]*Department of Physics, Columbia University, New York, NY 10027, USA*

[30]*Monash Centre for Astrophysics (MoCA), School of Physics and Astronomy, Monash University, VIC 3800, Australia*

[31]*Kavli institute for astronomy and astrophysics, Peking University, Beijing 100871, P. R. China*

[32]*National Radio Astronomy Observatory, PO Box 2, Green Bank, WV 24944, USA*

[33]*National Radio Astronomy Observatory, 520 Edgemont Rd, Charlottesville, VA 22903, USA*

[34]*TAPIR, California Institute of Technology, MC 350-17, Pasadena, CA 91125, USA*

[35]*Physics Department, Lafayette College, Easton, PA 18042, USA*

[36]*Physics Department, Texas Tech University, Box 41051, Lubbock, TX 79409, USA*

[37]*Department of Astronomy, University of Virginia, PO Box 400325 Charlottesville, VA 22904-4325, USA*

[38]*Université Paris-Diderot-Paris7 APC - UFR de Physique, Batiment Condorcet, 10 rue Alice Domont et Léonie Duquet, F-75205 Paris Cedex 13, France*

[39]*Centre for Astrophysics and Supercomputing, Swinburne University of Technology, PO Box 218, Hawthorn, VIC 3122, Australia*

[40]*School of Physics and Astronomy, University of Birmingham, Edgbaston, Birmingham B15 2TT, UK*

[41]*Center for Gravitation, Cosmology and Astrophysics, Department of Physics, University of Wisconsin-Milwaukee, PO Box 413, Milwaukee, WI 53201, USA*

[42]*Physics and Astronomy Department, Oberlin College, Oberlin, OH 44074, USA*

[43]*Department of Physics and Astronomy, University of New Mexico, Albuquerque, NM 87131, USA*

[44]*Laboratoire Univers et Théories LUTh, Observatoire de Paris, CNRS/INSU, Université Paris Diderot, 5 place Jules Janssen, F-92190 Meudon, France*

[45]*School of Physics, Huazhong University of Science and Technology, Wuhan, Hubei Province 430074, China*

[46]*School of Physics, University of Western Australia, 35 Stirling Hwy, Crawley, WA 6009, Australia*

[47]*School of Physical Science and Technology, Southwest University, Chongqing 400715, China*

This paper has been typeset from a T{}EX/L{}ATEX file prepared by the author.